



# AMERICAN METEOROLOGICAL SOCIETY

*Bulletin of the American Meteorological Society*

## **EARLY ONLINE RELEASE**

This is a preliminary PDF of the author-produced manuscript that has been peer-reviewed and accepted for publication. Since it is being posted so soon after acceptance, it has not yet been copyedited, formatted, or processed by AMS Publications. This preliminary version of the manuscript may be downloaded, distributed, and cited, but please be aware that there will be visual differences and possibly some content differences between this version and the final published version.

The DOI for this manuscript is doi: [10.1175/BAMS-D-12-00124.1](https://doi.org/10.1175/BAMS-D-12-00124.1)

The final published version of this manuscript will replace the preliminary version at the above DOI once it is available.



1 **A Drought Monitoring and Forecasting System for Sub-Sahara African Water**  
2 **Resources and Food Security.**

3  
4 Justin Sheffield<sup>1</sup>, Eric F. Wood<sup>1</sup>, Nathaniel Chaney<sup>1</sup>, Kaiyu Guan<sup>1</sup>, Sara Sadri<sup>1</sup>, Xing  
5 Yuan<sup>1</sup>, Luke Olang<sup>2</sup>, Abou Amani<sup>3</sup>, Abdou Ali<sup>4</sup>, Siegfried Demuth<sup>5</sup>, and Laban Ogallo<sup>2</sup>

6  
7 Submitted to the Bulletin of the American Meteorological Society

8 8 May 2013

9 Revised 16 September 013

10  
11 <sup>1</sup>Department of Civil and Environmental Engineering, Princeton University, Princeton,  
12 NJ, 08540, USA

13 <sup>2</sup>Intergovernmental Authority on Development (IGAD) Climate Prediction and  
14 Applications Center (ICPAC), Nairobi, Kenya

15 <sup>3</sup>UNESCO International Hydrological Programme (IHP), Nairobi, Kenya

16 <sup>4</sup>Centre Regional de Formation et d'Application en Agrométéorologie et Hydrologie  
17 Opérationnelle (AGRHYMET), Niamey, Niger

18 <sup>5</sup>UNESCO International Hydrological Programme (IHP), Paris, France

19  
20 Corresponding author:

21 Justin Sheffield

22 Department of Civil and Environmental Engineering,

23 Princeton University,

24 Princeton, NJ, 08540,

25 USA

26

27 **Capsule:** The development and implementation of a drought monitoring and seasonal  
28 hydrological forecast system for sub-Saharan Africa contributes to building capacity  
29 through technology and knowledge transfer.

30

31 **Abstract**

32

33 Drought is one of the leading impediments to development in Africa. Much of the  
34 continent is dependent on rain-fed agriculture, which makes it particularly susceptible to  
35 climate variability. Monitoring drought and providing timely seasonal forecasts are  
36 essential for integrated drought risk reduction. Current approaches in developing regions  
37 have generally been limited, however, in part because of unreliable monitoring networks.  
38 Operational seasonal climate forecasts are also deficient, often reliant on statistical  
39 regressions, which are unable to provide detailed information relevant for drought  
40 assessment. However, the wealth of data from satellites and recent advancements in large  
41 scale hydrological modeling and seasonal climate model predictions have enabled the  
42 development of state-of-the-art monitoring and prediction systems that can help address  
43 many of the problems inherent to developing regions. An experimental drought  
44 monitoring and forecast system for sub-Saharan Africa is described that is based on  
45 advanced land surface modeling driven by satellite and atmospheric model data. Key  
46 elements of the system are the provision of near real-time evaluations of the terrestrial  
47 water cycle and an assessment of drought conditions. The predictive element takes  
48 downscaled ensemble dynamical climate forecasts and provides, when merged with the  
49 hydrological modeling, ensemble hydrological forecasts. We evaluate the overall skill of  
50 the system for monitoring and predicting the development of drought, and illustrate the  
51 use of the system for the 2010/11 Horn of Africa drought. A key element is the transition  
52 and testing of the technology for operational usage by African collaborators and we  
53 discuss this for two implementations in West and East Africa.

54

55 **1. Introduction**

56 Drought is a naturally occurring climate phenomenon that impacts human and  
57 environmental activity globally and can be considered to be one of the costliest and  
58 widespread of natural disasters (NCDC, 2012; Below et al., 2007). One of the reasons for  
59 this is the often large spatial extent and lengthy duration of droughts, sometimes reaching  
60 continental scales and lasting for multiple years (Sheffield and Wood, 2011). Compared  
61 to other natural disasters, this translates into a greater proportion of the population  
62 affected. Drought can also be exacerbated by human activities such as deforestation, land  
63 use change and poor management of water resources that feedback to climate and alter  
64 the storage of water on the land. In sub-Saharan Africa (SSA), droughts account for less  
65 than 20% of natural disasters but account for over 80% of the affected population  
66 (UN/ISDR, 2007). Much of the continent is dependent on rain-fed agriculture, which  
67 makes it particularly susceptible to climate variability. Almost 70% of the labour force is  
68 engaged in agricultural work and agriculture contributes to about 25% of average GDP  
69 across the continent (Dixon et al., 2001). When the direct impacts of drought on  
70 agriculture and water resources occur over these large space and time scales there are  
71 deleterious effects on food and water security. The impacts are driven by the generally  
72 high vulnerability of the local populations and are exacerbated by prevailing local and  
73 external economic and political conditions (Haile, 2005), which can be associated with  
74 development of famine and may be accompanied by the spread of disease. Drought  
75 hampers efforts to reach the Millennium Development Goals (MDGs; UN, 2005) and is  
76 therefore one of the leading impediments to development in SSA (Benson and Clay,  
77 1998; Brown et al., 2011). The population of SSA is over 870 million people and is

78 expected to at least double by mid century. Coupled with expected overall drying with  
79 climate change, in particular in southern Africa and parts of West Africa (Sheffield and  
80 Wood, 2008; Williams and Funk, 2011; Seneviratne et al., 2012), there are worrisome  
81 implications for water resource sustainability and food security.

82 Sub-Saharan Africa has suffered from many devastating droughts in recent  
83 history. Among some of the most devastating droughts globally during the past 50 years  
84 have been the Sahelian droughts of the 1970s and 80s, which drove famine conditions  
85 over much of the region and led to an estimated 600,000 deaths (Benson and Clay, 1998;  
86 Mortimore and Adams, 2001) and droughts in 1991-92 in southern Africa (Benson and  
87 Clay, 1998). Most recently, multi-year droughts across the Horn of Africa (Lyon and  
88 DeWitt, 2012) led to food shortages across the region and famine conditions in Somalia  
89 and northern Kenya (UNOCHR, 2011) that have intensified the debate on the role of  
90 climate change and how drought will change in the future (Kotir, 2011).

91 Drought in SSA is linked to the high seasonal and inter-annual variability in  
92 rainfall as shown in Figures 1 and 2. In general, seasonal rainfall higher than 500 mm is  
93 required to sustain healthy agriculture, highlighting the tenuous nature of agropastoral  
94 livelihoods in many parts of SSA. Rainfall is highly seasonal with well-defined dry  
95 seasons across most of the continent. In West Africa, the rainy season is mainly  
96 concentrated in July-September with the northward movement of the West African  
97 Monsoon rains. This is also the case in the Horn of Africa, with some parts (Kenya,  
98 northern Tanzania) experiencing two peaks (short and long rains). In southern and east  
99 Africa the rainy season is generally from November to April. Variability at inter-annual  
100 and decadal time scales is large (Figure 2), especially in the transitional regions between

101 semi-arid and arid regions, such as the Sahel during the early growing season (June-  
102 August). Decadal persistence in wet or dry conditions is one of the greatest problems.  
103 Much of this variability is driven by connections to ENSO as well as to variations in the  
104 Atlantic and Indian Ocean (e.g. Rowell, 2013).

105

## 106 **2. The Need and Potential for Physically-Based Drought Monitoring and Prediction**

107 Monitoring drought development and providing timely seasonal forecasts are  
108 essential for drought risk reduction and especially in SSA where livelihoods are closely  
109 intertwined with climate variability (Tarhule and Lamb, 2003; Amisshah-Arthur, 2003;  
110 Hayes et al., 2004; Hansen et al., 2011; Pozzi et al., 2013). Current approaches in  
111 developing countries have generally been limited, in part because of unreliable  
112 monitoring networks and lack of access to information and technology that prevents the  
113 development of systems locally, as well as generally low institutional capacity and lack  
114 of national policy on drought mitigation. In SSA, regional climate outlook forums  
115 (RCOFs) were initiated in 1997 and have been the primary mechanism for generating and  
116 disseminating seasonal climate forecasts (Ogallo et al., 2008). These operational seasonal  
117 climate forecasts are reliant on statistical regressions and provide only a broad-brush  
118 view of seasonal rainfall (e.g. tercile probabilities), and are therefore unable to provide  
119 detailed information relevant for agricultural adaptation, such as start of the wet season,  
120 intra-seasonal rainfall, soil moisture and extreme temperatures (Patt et al., 2007). There is  
121 also a reported tendency for the consensus of the forums to hedge on the side of caution  
122 when issuing forecasts (Hansen et al., 2011). In several countries, the national  
123 meteorological and hydrological agencies extend the RCOF outlooks to provide local

124 interpretation and more detailed impact orientated information to farmers, subsistence  
125 communities and water resources managers. Nevertheless, the skill, resolution, and local  
126 relevance of the forecasts generally remain dependent on the RCOF outlooks, which may  
127 limit confidence and uptake of the forecasts (e.g. Manatsa et al., 2012).

128         The wealth of data from satellites and advancements in large scale hydrological  
129 modeling and seasonal climate model predictions have enabled the development of state-  
130 of-the-art monitoring and prediction systems in developed regions, such as the U.S. and  
131 Europe, that can help address many of the problems inherent to developing regions. For  
132 example, the U.S. Drought Monitor (Svoboda et al., 2002) and the European Drought  
133 Observatory (EDO; Vogt et al., 2011) combine bottom-up approaches of merging  
134 drought evaluations at national and sub-national levels with a top-down approach of  
135 providing continental scale information from meteorological networks, hydrological  
136 modeling and satellite remote sensing. In SSA, elements of these are mirrored by the  
137 Famine Early Warning System Network (FEWS-NET) and the FAO Global Information  
138 and Early Warning System on Food and Agriculture (GIEWS). These systems  
139 accumulate information from local observers, market reports and remote sensing on  
140 evolving drought and food security conditions and provide outlooks on potential problem  
141 areas.

142         Satellite remote sensing is a particularly promising source of information in SSA  
143 as it is possible to measure every component of the hydrological cycle at the land surface,  
144 and the state of natural vegetation and agriculture, often at very high spatial resolution (<  
145 1km) and in near real-time (Tang et al., 2009; Wardlow et al., 2012). Satellite-based  
146 retrievals for some variables are well developed (e.g. for precipitation, Huffman et al.,

147 2007; and vegetation, Funk and Brown, 2005) and are a promising new source of data for  
148 other variables (e.g. Gao et al., 2012; Tapley et al., 2004; de Jeu et al. 2008; Vinukollu et  
149 al., 2011). Their use in operational drought monitoring is still generally in its infancy,  
150 although a substantial body of research literature now exists on the potential for drought  
151 monitoring at large scales (e.g. Anderson et al., 2011; Houborg et al., 2012; Mu et al.,  
152 2013). The use of satellite remote sensing to augment low density in situ observations has  
153 obvious benefits, however there are several challenges that need to be addressed to  
154 realize their potential in the context of drought monitoring. In general, these include the  
155 relatively short record lengths of satellite products, changes in satellite sensors that can  
156 lead to temporal inhomogeneities, and the indirect nature of the retrievals of physical  
157 variables. In particular, errors in individual products, inconsistencies between products  
158 and non-closure of the water budget imply that they should be used with caution  
159 (Sheffield et al., 2009; Gao et al., 2010; Pan et al., 2012; Armanias and Fisher, 2013).

160 Remote sensing generally provides independent views of different parts of the  
161 coupled ecological-hydrological system. However, there is scope to provide a holistic and  
162 consistent view of drought by merging remote sensing data with land surface  
163 hydrological modeling, either directly via assimilation (e.g. satellite retrievals of soil  
164 moisture) or indirectly in the form of input drivers (e.g. precipitation or vegetation).  
165 Several studies have shown this potential (Brocca et al., 2010; Milzow et al., 2010; van  
166 Dijk and Renzullo, 2011; Anderson et al., 2013). Furthermore, land surface hydrological  
167 modeling has evolved to a state that models can provide realistic depictions of the water  
168 cycle over large scales with acceptable errors when driven by accurate meteorological  
169 data and/or merged with remote sensing data. Much of this progress has been derived

170 from regional and global intercomparison studies that have highlighted key model  
171 differences and provided mechanistic insights into model behavior and errors  
172 (Henderson-Sellers et al., 1993; Mitchell et al., 2004; Guo et al., 2006; Xia et al., 2012),  
173 as well as better input data. In particular, availability of real-time satellite precipitation  
174 data has enabled the use of hydrological models for flood and drought applications in  
175 regions of low density ground measurements (e.g. Pan et al., 2010; Yilmaz et al., 2011),  
176 although currently this approach does not out-perform those using just a handful of  
177 gauges (e.g. Stisen and Sandholt, 2010).

178         Seasonal hydrological predictions have the potential to provide vital information  
179 throughout SSA for a variety of needs including water resources management,  
180 agricultural and urban water supply and flood mitigation. In particular, seasonal forecasts  
181 of drought risk can enable farmers to make adaptive choices on crop varieties, labor  
182 usage, and technology investments (Hansen et al., 2011). Forecast skill is generally  
183 derived from teleconnections with ocean variability, in particular sea surface temperature  
184 (SST) anomalies, as well as persistence in the state of the land in terms of soil moisture,  
185 snowpack or streamflow conditions (Shukla et al., 2013). In particular, the persistence of  
186 SST anomalies forms the basis of climate forecasts either as a predictor in a statistical  
187 model or as boundary conditions to dynamic seasonal forecasts using General Circulation  
188 Models (GCM). For SSA, the main source of predictability is derived from the El Nino  
189 Southern Oscillation (ENSO) and its manifestation in SST anomalies in the eastern  
190 tropical Pacific ocean, with drought more likely over west Africa and southern Africa  
191 during El Nino events and over east Africa during La Nina events (Camberlin et al.,  
192 2001; Smith et al., 2012; Yuan et al., 2013; Rowell, 2013), although the spatial footprint

193 of these teleconnections may be limited (Yuan et al., 2013). Forecasts of hydrological  
194 variables can also be derived using hydrological models forced by statistical or dynamical  
195 precipitation forecasts. More often, operational systems are based on the use of Ensemble  
196 Streamflow Prediction (ESP) type forecasts, which sample from the historic climate  
197 record and rely mainly on the skill derived from the land surface initial conditions.  
198 Operational versions of such systems are generally limited to a few regions around the  
199 world, for example in the US, Europe and Australia, and are virtually absent in SSA.

200         Seasonal climate forecasts from dynamical models have evolved considerably  
201 over recent years and are now showing greater skill than statistical forecasts, at least for  
202 large-scale climate features such as ENSO (e.g. Jin et al., 2008; Weisheimer et al., 2009;  
203 Barnston et al., 2012). They also provide forecasts that are grounded in the physics of  
204 weather and climate, and therefore can provide objective information on multiple aspects  
205 of drought (for example, precipitation and temperature), in contrast to statistical  
206 prediction tools, which are generally limited to single variable outcomes. The challenge is  
207 that precipitation forecasts from these models are generally limited in skill beyond a few  
208 weeks because of the inherent chaotic nature of the atmosphere (Lavers et al., 2009; Yuan  
209 et al., 2011), and otherwise to regions with strong teleconnections with ENSO at seasonal  
210 time scales, and then only for coarse tendencies for drier or wetter conditions than  
211 normal. Furthermore, the model spatial resolution (of the order of hundreds of kms) is  
212 generally too coarse to be useful for hydrological prediction. Nevertheless, continued  
213 improvements in dynamical forecasts (Yuan et al., 2011; Pappenberger et al., 2011;  
214 Barsnton et al., 2012), the development of downscaling and bias correction  
215 methodologies for hydrological applications (Luo and Wood, 2008; Gobena and Gan,

216 2010) and the focus on improved estimates of initial conditions in lieu of forecast skill  
217 (Bierkins and van Beek, 2009; Li et al., 2009; Shukla et al., 2013; van Dijk et al., 2013)  
218 have provided incentive to develop and test experimental hydrological forecast systems.  
219 Despite the high frequency and impacts of drought on SSA populations, and the potential  
220 for increased resilience of local populations if monitoring and forecast information can be  
221 accessed and utilized, the evaluation and implementation of seasonal hydrological  
222 forecasts has been limited to a few regional (e.g. Oettli et al., 2011; Manatsa et al., 2012)  
223 and continental studies (e.g. Dutra et al., 2012b; Yuan et al., 2013).

224         This article presents the development and implementation of an African Drought  
225 Monitor (ADM), an advanced real-time drought monitoring and seasonal forecast system  
226 for sub-Saharan Africa, which has evolved via collaboration with the UNESCO  
227 International Hydrological Programme (IHP). The IHP supports an international  
228 scientific cooperative program in water research, education and capacity building  
229 responding to the growing needs of sustainable development. In 2006, IHP discussed the  
230 possibility of developing a demonstration system for SSA that would respond to the  
231 needs of UNESCO members, contribute to IHP activities and capacity building, and  
232 respond to the drought needs of the Group on Earth Observations (GEO). The initial  
233 demonstration system has now matured into an operational framework that merges  
234 statistical and dynamical climate predictions, hydrological models and remote sensing  
235 data to provide timely and useful information on drought in SSA. The system has been  
236 implemented at regional centers in Niger and Kenya and the article highlights the  
237 feedback with local meteorologists and hydrologists who are charged with managing  
238 local water resources systems and providing information to farmers.

239

### 240 **3. Sub-Saharan African Drought Monitoring and Seasonal Forecast System**

241

#### 242 *3.1. Overview of Approach*

243         The system estimates drought conditions through a combination of hydrological  
244 modeling, satellite remote sensing and seasonal climate forecasts. It draws from the long  
245 legacy of operational and experimental systems in the U.S., in particular the Princeton  
246 drought monitoring and forecast system (Luo et al., 2007) that was developed within the  
247 North American Land Data Assimilation System Phase 2 (NLDAS-2; Xia et al., 2012)  
248 and the NCEP Climate Test Bed program. The system consists of three parts (Figure 3):  
249 First, a historic, multi-decadal reconstruction of the terrestrial water cycle is obtained by  
250 forcing the Variable Infiltration Capacity (VIC) land surface hydrological model (Liang  
251 et al. 1996) with a merged reanalysis/observation data set. This forms the climatology  
252 against which current conditions are compared. Second, the real-time monitoring system  
253 (2009-present) is driven by remotely sensed precipitation and atmospheric analysis data  
254 that tracks drought conditions in real-time. The simulated outputs are augmented by  
255 satellite remote sensing of soil moisture and vegetation indices. Third, a seasonal forecast  
256 component provides hydrological predictions and derived drought products out to 6-  
257 months, based on bias-corrected and downscaled climate model forecasts that are used to  
258 drive the VIC model.

259

#### 260 *3.2. Hydrological Modeling and Data Sources*

261           The VIC model is used to predict land surface hydrological fluxes and states. VIC  
262 is a semi-distributed, grid-based model that represents sub-grid variability in land cover,  
263 elevation, soil water storage capacity and storm coverage. The model is run in two  
264 simulation modes: retrospectively and in near real-time. The retrospective simulation  
265 mode forms a long-term climatology to which current conditions from the real-time mode  
266 can be compared. The retrospective simulation covers the period 1950-2008 and is forced  
267 by the long-term global meteorological forcing dataset of Sheffield et al. (2006), which  
268 merges gridded observational data with satellite remote sensing products and atmospheric  
269 reanalysis data. This dataset has been downscaled to 0.25-degree resolution and is  
270 currently being updated based on improved assimilation of station data (Chaney et al.,  
271 2013).

272           The real-time simulation is forced by a combination of precipitation from the  
273 Tropical Rainfall Measurement Mission (TRMM) Multi-Satellite Precipitation Analysis  
274 (TMPA; Huffman et al., 2007) and temperature and windspeed from the NOAA NCEP  
275 Global Forecasts System (GFS). Other required variables (surface solar and longwave  
276 radiation; humidity, pressure) are predicted from the precipitation and temperature data  
277 using empirical regressions (Bohn et al., 2013). The satellite-based TMPA and GFS data  
278 are bias-corrected based on climatological differences with the long-term dataset for their  
279 overlap period (approximately 2002-2008) by matching their empirical cumulative  
280 probability distribution functions. We evaluated the robustness of this approach by  
281 comparing the historic simulation with a simulation forced by the bias-corrected TMPA  
282 data for the overlap period. This showed relative biases of less than 1 percent in predicted  
283 runoff and soil moisture averaged over large river basins such as the Niger and Congo.

284 Boundary conditions for the model include the land cover map based on  
285 Advanced Very High Resolution Radiometer (AVHRR) data (Hansen et al., 2000), and  
286 soil type and texture based on the FAO digital soil map of the world (FAO, 1995). The  
287 model was calibrated against streamflow observations from 966 stations of the Global  
288 Runoff Data Center (GRDC) across SSA, filtered for upstream dams. The GRDC stream  
289 gauge database over the continent was disaggregated into gridded monthly runoff fields  
290 over the entire domain (Chaney and Sheffield, 2012). Following Troy et al. (2008), the  
291 VIC model is calibrated at each grid cell against the derived runoff fields between 1970  
292 and 1990 using the Shuffled-Complex evolution algorithm (Duan et al. 1992).

293

### 294 *3.3. Other Data Products*

295 The system is flexible enough to incorporate other sources of data including  
296 output from other models and remote sensing. Currently, remotely sensed soil moisture  
297 and vegetation data are included in the system to complement the modeled information.  
298 Data from the Soil Moisture Ocean Salinity (SMOS) L-band upwelling passive  
299 microwave sensor are included in the system in the form of a soil moisture index (Kerr et  
300 al., 2012). This dataset has been initially evaluated by Al-Bitar et al. (2012) and Pan et al.  
301 (2012) over the US and by Gruhier et al. (2013) for West Africa, and shows promise for  
302 drought monitoring (Sahoo et al., 2011) as a complement to the modeled output, as well  
303 as to provide corrections to the satellite rainfall (e.g. Pellarin et al., 2008; Crow et al.,  
304 2011) or directly via assimilation (Sahoo et al., 2012).

305 The system also displays operational retrievals of vegetation stress from visible  
306 and microwave sensors drawing from the distinctive and complementary information that

307 each provides about vegetation (Guan et al., 2012). The optical-based vegetation index  
308 (VI) product captures the landscape-integrated canopy-level leaf chlorophyll and  
309 photosynthetic intensity (Sellers et al., 1992). It is based on a merging of the GIMMS  
310 NDVI for the historic period (1982-2008) and the MODIS EVI for 2000-present. The  
311 passive microwave based vegetation optical depth (VOD) product captures the landscape-  
312 integrated total water column through the whole canopy (Jones et al., 2012). It is  
313 composed of the VOD product of Liu et al. (2011) based on SSM/I, TRMM and AMSR-  
314 E for 1987-2008, and the AMSR-E based VOD (Jones and Kimball, 2012). A third  
315 product based on scatterometer backscatter (dB) captures the landscape-integrated  
316 vegetation canopy biomass (depending on the penetration of the wavelength) and top-  
317 canopy water content (Jarlan et al., 2002). In our case, we merged the Ku-band dB from  
318 QuickSCAT (2000-2009) and C-band dB from ASCAT (2009-present) using the quantile  
319 matching approach. The Ku-band dB only detects the top-canopy information due to its  
320 relatively small wavelength (13GHz), whereas the C-band dB (6GHz) penetrates the  
321 canopy and captures information about both surface soil moisture and vegetation states  
322 (Guan et al., 2013).

323

#### 324 *3.4. Seasonal Drought Forecasts*

325 The seasonal forecast system is based on climate forecasts from the NCEP  
326 Climate Forecast System version 2 (CFSv2; Saha et al., 2013, submitted to Journal of  
327 Climate), which is the second generation system from the CFSv1 (Saha et al., 2006). The  
328 CFSv2 improves on the previous version through upgraded physical parameterizations  
329 and data assimilation scheme. The precipitation and temperature forecasts from CFSv2

330 show a significant improvement over CFSv1 (Yuan et al., 2011). Monthly precipitation  
331 and temperature at the CFSv2 model scale are bias corrected and downscaled using a  
332 Bayesian merging method (Luo et al., 2007, 2008) to 0.25-degree, daily resolution. These  
333 data are then used to force the VIC model to generate the hydrologic forecasts.

334

### 335 *3.5. Hydrological and Drought Products*

336 A suite of drought indices is produced by the system (Table 1) that reflects  
337 different aspects of drought. The standardized precipitation index (SPI; McKee et al.,  
338 1993) is the World Meteorological Organization (WMO) ratified index for  
339 meteorological drought. The current SPI-n value is calculated by considering data from  
340 the current and n-1 preceding months. The forecasted SPI-n values are calculated in the  
341 same way and may contain historic data depending on the forecast lead-time and value of  
342 n (Quan et al. 2012; Yoon et al. 2012; Yuan and Wood 2013). The antecedent historic  
343 data can be considered as information from initial conditions in the same way as other  
344 drought indices based on land surface hydrological variables, such as soil moisture. The  
345 soil moisture index is based on the percentile index of Sheffield et al. (2004) developed  
346 for the continental US and previously applied regionally (e.g. Wang et al., 2011) and  
347 globally (e.g. Sheffield et al., 2009). The index is calculated by determining the percentile  
348 of the daily average of relative soil moisture at each grid cell with respect to its empirical  
349 cumulative probability distribution function provided by the historical simulations (1950-  
350 2008). The cumulative streamflow index represents the volume deficit below the median  
351 flow (Tallaksen and van Lanen, 2004) and is calculated at 822 streamflow gauging points  
352 across SSA. The vegetation indices are based on the visible and microwave data products

353 and are calculated as percentiles, similar to the soil moisture. Each of the indices  
354 represents a normalized representation of the variable that is calculated relative to the  
355 long-term climatology from the retrospective simulation. The ~60-year climatology is  
356 long enough to contain several extreme drought events such as those of the 1970s and  
357 1980s in the Sahel, and in the 1990s in southern Africa, and therefore provides a robust  
358 climatology. Extending the dataset to the earlier part of the instrumental record would  
359 include more extreme events but this is only possible for some regions with adequate  
360 station density. The drought indices (and all hydrological variables and meteorological  
361 forcings) are available for the entire record between 1950 and real-time.

362

### 363 *3.6. Web Interface*

364 A key element of the system is the provision of an intuitive and easy to use web  
365 interface to allow users to view the predictions and extract data for further analysis.  
366 Figure 4 shows a snapshot of the interface showing recent soil moisture conditions. The  
367 interface is based on Google Maps®, which provides the Geographical Information  
368 System (GIS) capabilities for panning and zooming, and overlaying other geographic  
369 layers, such as political boundaries, towns and cities, and satellite land cover imagery.  
370 The system features a simple and intuitive user interface that allows the user to access  
371 different hydrological and drought products as spatial maps. The user can display current  
372 conditions or animate a series of maps to show evolving conditions. Streamflow drought  
373 can also be displayed for over 822 gauges that correspond to the GRDC network and  
374 FAO reservoir database. These gauges were chosen to coincide with actual gauging  
375 locations that are or were active. Other locations can be added where necessary at gauged

376 or ungauged locations. The user can also drill down to examine the water budget and  
377 drought indices averaged over the upstream river basin by clicking on a stream gauge  
378 (see Figure 4). Given the large spatial domain and potential diversity of users, the system  
379 also features multi-lingual support, currently for English, French, Arabic, Mandarin and  
380 Spanish. The interface can be accessed at <http://hydrology.princeton.edu/adm>. The  
381 drought indices output by the system are also provided as an Open Geospatial Compliant  
382 web service that can be picked up by other organizations to produce, for example,  
383 blended drought indicators such as provided by the US Drought Monitor. Currently the  
384 soil moisture drought index is served to the NOAA National Climatic Data Center to  
385 provide coverage for the African continent for the Global Drought Monitor Portal (Heim  
386 and Brewer, 2012).

387

#### 388 **4. Transition to African Regional Centers**

389 In 2012, the system was transitioned and tested for operational usage by African  
390 collaborators at workshops held in two regional centers in SSA. The goals of the  
391 workshops were to understand user needs for drought information, current capabilities of  
392 regional centers and national agencies for providing climate and hydrological  
393 information, and training and feedback on the system, including design and  
394 implementation of regional validation plans. The drought monitor software and data were  
395 installed on center servers and hydrological scientists and professionals were trained in  
396 the operational running of the system and interpretation of the data output. Feedback was  
397 also solicited from scientists and managers from national hydrological, meteorological  
398 and agriculture agencies and services. The first workshop was held in January 2012 at the

399 AGRHYMET (Centre Regional de Formation et d'Application en Agrométéorologie et  
400 Hydrologie Opérationnelle) regional center in Niamey, Niger (Figure 5a), which provides  
401 information and training in support of improved agricultural production and food security  
402 for CILSS member countries of Burkina Faso, Cape Verde, Chad, Gambia, Guinea  
403 Bissau, Mali, Mauritania, Niger, and Senegal. Feedback from this workshop was vital to  
404 understand the utility of the system, from the point of view of users from the  
405 meteorological and hydrological communities who saw the potential of the historic and  
406 real-time data at ungaged locations and from the point of view of managers who saw the  
407 potential of the system for decision-making. A key lesson learnt was that providing a  
408 working system was essential to show the potential for management and research, but one  
409 that could then be tailored to local user needs and was validated to ensure confidence in  
410 the data and uptake of the information. Feedback from participants also highlighted the  
411 pressing need for a predictive component for water resources and agricultural planning  
412 and hazard mitigation. The second workshop was held in June 2012 at the  
413 Intergovernmental Authority on Development (IGAD) Climate Prediction and  
414 Applications Center (ICPAC) in Nairobi, Kenya (Figure 5b), which disseminates  
415 information to countries within the Greater Horn of Africa (Djibouti, Eritrea, Ethiopia,  
416 Kenya, Rwanda, South Sudan, Sudan, Somalia, Tanzania, Uganda). Both workshops  
417 developed a validation plan as an outcome, the results of which are shown below for the  
418 ICPAC workshop.

419 A third workshop is expected to take place at AGRYHMET in late 2013 with the  
420 goals of strengthening capacity and long-term sustainability in use of the system, and in  
421 particular the seasonal forecasting component that was developed since and in response

422 to the first workshop in January 2012. User needs will be focused on the point of view of  
423 women and youth who are generally under-represented but particularly vulnerable to  
424 drought impacts, with the goal of mainstreaming their engagement in understanding user  
425 needs and developing drought policies. Policy makers will be invited to discuss drought  
426 management issues through plans and policy recommendations, including the kinds of  
427 institutional settings that are required. The workshop will also focus on user needs and  
428 alternative information pathways for dissemination of data, as well as to revisit validation  
429 and operational aspects of the system.

430

## 431 **5. Validation and Results**

432

### 433 *5.1. Overview of Performance of the VIC Model*

434 Figure 6 shows a summary of large-scale evaluations of the bias-corrected  
435 satellite precipitation and the VIC model output against available observational and other  
436 model-based data. Evaluations at this scale provide confidence in the overall approach of  
437 using satellite-based products and hydrological models as surrogates for ground  
438 measurements of hydrological variables. The lynchpin of the system is the accuracy of  
439 the satellite precipitation. Improvements in the TMPA product have led to several  
440 updates in its real-time and historical research products (e.g. Zhou et al., 2013), and the  
441 real-time product is now calibrated based on climatological evaluations against monthly  
442 gauge analyses. Sylla et al. (2012) evaluated the TMPA (3B42 V6) dataset for Africa and  
443 showed that the large-scale patterns of precipitation were similar to observational  
444 estimates from GPCP and FEWS products but there were considerable differences

445 between all datasets in terms of daily higher order statistics, such as extreme rainfall and  
446 the duration between rain events. Of particular importance is the latter, which the TMPA  
447 overestimates and this is corrected for in the system based on the historical gauge based  
448 climatology. Figure 6a-c shows that, in general, the real-time TMPA (3B42RT V6) are  
449 biased high annually compared to our long-term observational dataset, despite the  
450 calibration. The bias is corrected for at monthly scale to ensure consistency between the  
451 historic and real-time predictions.

452 Figure 6d-f shows an evaluation of the VIC output for simulated streamflow  
453 against 624 station time series from the GRDC database. The figure highlights the  
454 scarcity of readily available data for many parts of the continent and especially in humid  
455 regions of central Africa and the drier greater Horn of Africa. The uncalibrated model  
456 shows large errors in terms of the Nash Sutcliffe efficiency (NSE; Nash and Sutcliffe,  
457 1970), especially in Cameroon and Gabon, with negative values indicating that the model  
458 does not perform better than the mean. The median NSE values increase after calibration  
459 from -0.04 to 0.93 and the mean from -0.54 to 0.66. In particular, the model simulations  
460 are improved across West Africa and East Africa, but stations in drier regions such as the  
461 Horn of Africa and southwest Africa show little improvement. The spatial distribution of  
462 the calibrated parameters generally reflects climate gradients for parameters that control  
463 baseflow and infiltration, but with random structure in the other parameters that reflects  
464 the many degrees of freedom in the calibration process.

465 The model output was also evaluated for consistency against satellite based  
466 evapotranspiration and land water storage change (Figure 6g-l). Evapotranspiration is  
467 from the RS-PM algorithm with the surface resistance parameterization of Mu et al.

468 (2007) as implemented by Vinokullo et al. (2012). This algorithm uses the same Penman-  
469 Monteith approach as the VIC model to estimate potential evaporation but differs in its  
470 representation of surface resistances, which are based on relationships with humidity and  
471 temperature. The evapotranspiration is compared for the annual mean over 1997-2006  
472 and shows similar spatial distribution and magnitudes but with large ( $> 1$  mm/day)  
473 negative differences in West Africa and the Ethiopian highlands, and positive differences  
474 in parts of the northern Congo. A lack of observational based estimates of  
475 evapotranspiration (except for a handful of flux measurement towers) means that the  
476 validation of the model simulation is difficult. The change in seasonal water storage is  
477 from the Gravity Recovery and Climate Experiment (GRACE) satellite and is calculated  
478 as the difference in the maximum and minimum seasonal water storage averaged over  
479 2003-2011. The comparison shows consistency between the datasets, given the  
480 differences in representative scale (GRACE represents variations on scales of about  
481 500km) and physical quantities represented (GRACE represents total water storage,  
482 including surface water, soil moisture, groundwater; VIC represents soil moisture only).  
483 The VIC data tend to underestimate the seasonal change across north central and central  
484 Africa, which may be a reflection of the current lack of groundwater representation in the  
485 model as north-central Africa has relatively shallow groundwater tables (MacDonald et  
486 al., 2012), current lack of representation of inland water bodies and wetlands or  
487 uncertainties in rainfall, particularly over central Africa.

488

489 *5.2. User Driven Validation: Example for Greater Horn of Africa*

490 Driven by feedback from the workshops and the need to evaluate the system for  
491 potential use in specific regions, a validation plan was developed that centered on  
492 hydrological validation at gauging sites of interest. National representatives were eager to  
493 understand the utility of the system, in particular for providing predictions at ungauged or  
494 no longer reporting locations. It was agreed at the workshops that more detailed  
495 evaluations at existing sites would be necessary to understand utility. Figure 7 shows  
496 results from the validation exercise for sites in the Greater Horn of Africa region for  
497 which data were supplied by participating national hydrological agencies at the ICPAC  
498 workshop. These sites were chosen because of the available data and key locations for  
499 supporting decision making in the various countries. None of these sites are available in  
500 the GRDC database, and so did not contribute to model calibration. The sites represent a  
501 mixture of basin sizes from 100 to 150,000 km<sup>2</sup>. The sites therefore provide a stringent  
502 test of the system for sites of particular interest to users. The results are mixed as  
503 expected given the low density of rain gauge data and the reliance on satellite  
504 precipitation since 2009, but are encouraging for most of the sites in terms of the  
505 depiction of a range of flows (mean daily flows, 3-day peak values and 7-day low flows)  
506 and the maintenance in the level of skill into the real-time period. However, some of the  
507 sites appear to be highly regulated by natural wetlands/lakes (e.g., the Kapiri site in  
508 Uganda that sits between two lakes) or potential water withdrawals. Overall, there is a  
509 tendency to over predict the different flow types in the larger/wetter basins and under  
510 predict in the smaller basins. The high bias suggests one or more problems related to the  
511 modeling framework, including over-estimation by the bias-corrected satellite  
512 precipitation, underestimation of evapotranspiration potentially due to upstream wetlands

513 and lakes that are not modeled (also leading to a lack of attenuation of flows), and lack of  
514 representation of anthropogenic impacts, such as water withdrawals. Accounting for  
515 withdrawals is challenging without direct information on withdrawals and irrigation, and  
516 current information is generally limited to national statistics. However, simple bias  
517 adjustment or even modeling of withdrawals could be implemented to better represent  
518 these local conditions.

519

### 520 *5.3. Seasonal Forecasts Evaluations*

521 The skill of the CFSv2 forced hydrological forecasts have been evaluated by  
522 Yuan et al. (2013) who analyzed a 26-year (1982-2007) set of seasonal hydrological  
523 hindcasts. They found that probabilistic drought forecasts of the 6-month SPI and soil  
524 moisture percentiles performed better than climatology over drier regions out to 3-5  
525 months, with SPI6 generally more skillful than soil moisture, except at the beginning of  
526 the rainy season in western and southern Africa because of the strength of the seasonal  
527 cycle. Similar results were found by Dutra et al. (2012b) based on evaluations of the  
528 ECMWF seasonal forecasts system of SPI over selected African river basins, but that  
529 skill generally increased with longer time scales of SPI. Figure 8 summarizes the skill of  
530 the CFSv2 driven hydrological forecasts for the start of wet season for three regions in  
531 terms of Brier skill scores (BSS) for 1, 2 and 3-month forecasts of soil moisture, from the  
532 beginning of the wet season. A BSS value of one indicates a perfect forecasts and zero  
533 indicates no skill relative to a climatological forecast. The scores are very high in parts of  
534 the regions that experience a later onset of the wet season (for example, in the northern  
535 Sahel), but are overall modest for lead-1 forecasts (Brier skill scores  $< 0.6$ ). At lead times

536 of 2 and 3 months, the scores drop to  $< 0.4$ , and less than zero in some areas indicating  
537 that the forecasts are worse than climatology. Examination of the time series of regional  
538 skill shows larger variability from year to year at longer lead times (not shown) and hints  
539 that slightly higher skill is associated with ENSO: for east Africa during La Niña events  
540 and for southern Africa during El Niño events.

541

## 542 **6. Case Study of the 2010-2011 Horn of Africa Drought**

543 The Horn of Africa (HoA) drought during 2010-2011 caused devastating human  
544 impacts across the region, in particular affecting southern Somalia, where an estimated  
545 250,000 deaths were associated with severe food insecurity and declared famine  
546 conditions, with over half of the deaths to children less than 5 years old (FAO, 2013).  
547 Although, the famine was a result of many factors, including the ongoing conflict and  
548 political insecurity in the region (Maxwell and Fitzpatrick, 2012), the drought played a  
549 major role. Figure 9 shows the output from the ADM for 2010-2011 for precipitation  
550 (expressed as SPI3), and soil moisture, vegetation and streamflow, expressed as  
551 percentile indices. The SPI3 shows the decline into drought conditions with the failure of  
552 the short-rains of the *deyr*-season at the end of 2010 (October-December) that was  
553 associated with the La Nina of 2010/11 (Dutra et al., 2012a; Lyon and DeWitt, 2012).  
554 The long-rains of the *gu*-season (April-June) of 2011 compounded the 2010 short-rains  
555 failure but were not as bad. Peak drought conditions were reached in about June 2011.  
556 The soil moisture and vegetation indices follow the decline in precipitation but with  
557 lagged response as the drought signal propagates through the system. The EVI shows the  
558 quickest response of the vegetation indices followed by the VOD and dB indices. The

559 peak spatial extent covered much of the region, from central Kenya up through southern  
560 Somalia and into southeastern Ethiopia, with most of the southeastern part of the region  
561 in drought conditions below the 20<sup>th</sup> percentile. The streamflow time series for the  
562 Shebelle River (Figure 9) indicates the local effect of the drought on one of southern  
563 Somalia's main rivers, which is an important source of water for irrigation and pastoral  
564 communities.

565 Figure 10 shows the 6-month hydrological forecasts for 10 ensemble members  
566 initialized on two dates: September 2010 (September-February) and February 2011  
567 (February-July). The forecasts, using procedures described earlier, are shown in terms of  
568 the area averaged soil moisture percentiles and the area in drought calculated for the main  
569 drought region (40-52E, 5-12N), which is also the same region used by Dutra et al.  
570 (2012a). The area in drought is calculated using a drought threshold of the 20<sup>th</sup> percentile  
571 of soil moisture. The September 2010 forecasts indicate good skill in reproducing the  
572 decline in soil moisture over the 6-months of the forecast, but under-predict the drought  
573 in latter months (Dec 2010 – Feb 2011). Furthermore, the spread across ensemble  
574 members is relatively small. The February 2011 forecasts also do well for the first two  
575 months (Feb-Mar 2011), showing an increase in drought, but then fail to show the  
576 continuation to the peak in April-June, with large spread among ensemble members.  
577 Dutra et al. (2012a) showed similar results in terms of precipitation using the ECMWF  
578 seasonal forecast system.

579

## 580 **7. Challenges and Future Directions**

581           Given the tremendous impact of drought in sub-Saharan Africa where the  
582 growing population is mostly dependent on rain-fed agriculture, the development and  
583 implementation of the ADM system has the potential to build capacity through  
584 technology and knowledge transfer. The feasibility of the system and its capability to  
585 monitor and forecast over large scales and at high resolution has been made possible with  
586 the advent of mature remote sensing data products and advances in land-surface modeling  
587 and seasonal dynamical forecasting, albeit subject to errors in the predictions as discussed  
588 previously. In particular, remote sensing is capable of overcoming sparse in-situ  
589 monitoring and differences in data availability across political boundaries that have  
590 historically hindered monitoring of regional phenomena such as drought.

591           The system shows encouraging performance at large-scale when compared to  
592 other estimates of the land water cycle, but notable errors when compared to local  
593 measurements. This is to be expected given the low density of monitoring networks, the  
594 high spatial and temporal variability of precipitation and the heterogeneity of the land  
595 surface, as well as human influences, such as water and land management. Currently the  
596 system does not simulate surface water bodies, such as lakes and wetlands, although  
597 these are features of the VIC model. Inclusion of these would be relatively  
598 straightforward and could potentially help improve performance at, for example, the  
599 stream gauging sites shown in the validation that are controlled by upstream wetlands and  
600 lakes. The system also does not account for human influences on water, such as  
601 reservoirs, river withdrawals and irrigation applications and return flows. Simple  
602 representations of these activities have been implemented in large-scale models (e.g.  
603 Haddeland et al., 2007), but further research is required to determine the best way to

604 implement these in the system, given the spatial diversity of practices and the low  
605 availability of estimates of water use. Continued collaboration with local partners is  
606 essential for conveying the current limitations of the system to users and the implications  
607 for decision making, and for making progress towards addressing these limitations  
608 through integration of local knowledge and information about water use.

609 Performance of the system is also highly reliant on the accuracy of the  
610 meteorological data. There is scope to enhance the accuracy of both the long-term data  
611 and real-time satellite-based data by merging with data from regional/national station  
612 databases (Chaney et al., 2013), other gauge/remote sensing analyses (e.g. FEWS) and  
613 with assimilation of remotely sensed soil moisture as a surrogate for on the ground  
614 rainfall where gauge data are unavailable (Pellarin et al., 2012). These enhancements will  
615 filter down into the seasonal forecasting component for which much of the skill in the  
616 first month is dependent on the initial conditions, which can also be improved through  
617 real-time assimilation of remotely sensed soil moisture and lake/river levels.

618 The seasonal hydrological forecasts show encouraging skill in the first one to  
619 three months depending on the region and season but are inherently limited by the chaotic  
620 nature of the atmosphere. Nevertheless, the case study of the 2010/11 Horn of Africa  
621 drought exemplifies the potential that large-scale teleconnections such as ENSO can  
622 provide extended and useful forecasts out to several months. The forecast system can be  
623 enhanced through use of climate forecasts from multiple models (both dynamical and  
624 statistical), drawing from strengths in each one, as has been demonstrated in other  
625 applications (e.g. Luo et al., 2007), as well as the potentially higher forecast skill  
626 conditional on climate states such as ENSO. Of particular importance is that the

627 hydrological predictions provide information on quantities, such as soil moisture and  
628 streamflow, and at spatial and temporal resolutions, that are relevant to end-users. We are  
629 currently adding an agricultural model to the forecast system, which when merged with  
630 the real-time vegetation indices, can provide crop yield forecasts.

631         Implementation of the system at regional centers in Niger and Kenya has  
632 highlighted the potential to augment existing capability in regions with established  
633 monitoring networks and provide the only source of information in areas lacking  
634 observations. It is important to recognize, however, that the sustainability of the system is  
635 highly dependent on the capacity of scientists and professionals who are charged with  
636 maintaining and running the system, and interpreting and disseminating the real-time  
637 updates and forecasts. It was therefore important to identify key personnel at regional  
638 centers and national agencies, and work with established researchers at affiliated  
639 universities, whilst at the same time training new young scientists and professionals.  
640 Experience has shown that ongoing collaborations through workshops, exchanges and  
641 educational activities provide the best means of sustained usage and further development  
642 of tailored regional systems. In this spirit, the system is open-source and free to use to  
643 encourage opportunities for further implementation, development and collaboration, and  
644 this is happening with ongoing validation activities for countries within the ICPAC and  
645 AGRHYMET regions. Direct funding for the development and implementation of the  
646 ADM was based solely on travel support and modest initial development funding from  
647 UNESCO IHP but leveraged other funding that supported the development of general  
648 methodologies for forecasting and modeling. Sustained funding is required to keep  
649 momentum going, train each new wave of scientists and professionals, and facilitate

650 long-term collaborations with African universities and training centers to build long-term  
651 capacity in research and development.

652         The application of hydrological and climate research into transferable technology  
653 with minimal overhead has been made possible with the development of the ADM and  
654 has the potential to help reduce the impacts of drought across sub-Saharan Africa.  
655 Realizing this potential, however, requires overcoming the many barriers that hinder the  
656 uptake and utility of output from the system, especially for local farming and pastoral  
657 communities. These barriers relate to the relevancy of the information to end users, the  
658 robustness of forecasts, and the communication and interpretation of information  
659 (Roncoli, 2006; Patt et al., 2007), especially given the current errors and uncertainties in  
660 the information from the ADM at local scales. Beneficial outcomes have been  
661 demonstrated in a few studies at local scale whereby changes in behavior based on  
662 forecast information brought about modest improvements in livelihoods, however the  
663 complexity of socio-economic contexts ensures that the benefits are difficult to reap (e.g.  
664 Ingram et al., 2002; Luseno et al., 2003; Ziervogel and Calder, 2003; Ziervogel et al.,  
665 2010; Roncoli et al., 2011). The potential at larger scales has yet to be realized (Tarhule  
666 and Lamb, 2003; Patt et al., 2007; Webster and Jian, 2011; Webster, 2013) and requires  
667 concerted efforts to bridge the gap between the wealth of physical climate, water and  
668 agricultural information and on-the-ground improvements in water and food security.

669

## 670 **Acknowledgements**

671         The authors acknowledge the support of the UNESCO International Hydrology  
672 Program (IHP) for supporting the initial development of the system, training workshops

673 and exchange visits. We also acknowledge the NOAA Climate Program Office  
674 Modeling, Analysis, Predictions and Projections (MAPP) Program that supported work  
675 on the forecast methodologies under grants NA11OAR4310097 and NA10OAR4310130.  
676 We thank Peris Muchiri of the FAO Somalia Water and Land Information Management  
677 (SWALIM), Nebert Wobusobozi, Director of Uganda Water Resources, and Gérard  
678 Ntungumburanye, Head of Hydrology Service at the Geographic Institute of Burundi  
679 (IGEBU) who provided the observed streamflow data used in the validation.  
680

681 **References**

682

683 Al-Bitar, A., D. Leroux, Y. Kerr, O. Merlin, P. Richaume, A. K. Sahoo, and E. F. Wood,  
684 2012: Evaluation of SMOS soil moisture products over continental US using the  
685 SCAN/SNOTEL network. *IEEE Transactions on Geosciences and Remote Sensing*,  
686 50, 1572-1586. doi:10.1109/TGRS.2012.2186581.

687 Amissah-Arthur, A., 2003: Targeting climate forecasts for agricultural applications in  
688 sub-Saharan Africa: situating farmers in user-space. *Climatic Change*, 58 (20).

689 Anderson, M. C., C. Hain, B. Wardlow, A. Pimstein, J. R. Mecikalski, and W. P. Kustas,  
690 2011: Evaluation of drought indices based on thermal remote sensing of  
691 evapotranspiration over the Continental United States. *J. Climate*, 24, 2025–2044.  
692 doi: <http://dx.doi.org/10.1175/2010JCLI3812.1>

693 Anderson, W. B., B. F. Zaitchik, C. R. Hain, M. C. Anderson, M. T. Yilmaz, J.  
694 Mecikalski, and L. Schultz, 2012: Towards an integrated soil moisture drought  
695 monitor for East Africa. *Hydrol. Earth Syst. Sci. Discuss.*, 9, 4587-4631,  
696 doi:10.5194/hessd-9-4587-2012.

697 Armanios, D. E., and J. B. Fisher, 2013: Measuring water availability with limited ground  
698 data: assessing the feasibility of an entirely remote-sensing-based hydrologic budget  
699 of the Rufiji Basin, Tanzania, using TRMM, GRACE, MODIS, SRB, and AIRS.  
700 *Hydrological Processes*, 27, 9.

701 Barnston, A. G., M. K. Tippett, M. L. L'Heureux, S. Li, and D. G. DeWitt, 2012: Skill of  
702 Real-Time Seasonal ENSO Model Predictions during 2002 to 2011: Is Our Capability  
703 Increasing?. *Bull. Amer. Meteor. Soc.*, 93, 631-651

704 Below, R., E. Grover-Kopec, M. Dilley, 2007: Documenting drought-related disasters: a  
705 global reassessment. *J. Environment and Development*, 16 (3), 328-344.

706 Benson, C., and E. Clay, 1998: The impact of drought on sub-Saharan African  
707 economics: A preliminary examination. World Bank Tech. Paper No. 401, 80 pp.

708 Bierkens, M. F. P., and L. P. H. van Beek, 2009: Seasonal Predictability of European  
709 Discharge: NAO and Hydrological Response Time, *J. Hydromet.*, 10(4), 953-968.

710 Bohn, T. J., B. Livneh, J. W. Oyler, S. W. Running, B. Nijssen, and D. P. Lettenmaier,  
711 2013: Global evaluation of MTCLIM and related algorithms for forcing of ecological  
712 and hydrological models. *Agr. Forest. Meteorol.*, 176, 38-49,  
713 doi:10.1016/j.agrformet.2013.03.003.

714 Brocca, L., F. Melone, T. Moramarco, W. Wagner, V. Naeimi, Z. Bartalis, and S.  
715 Hasenauer, 2010: Improving runoff prediction through the assimilation of the  
716 ASCAT soil moisture product. *Hydrology and Earth System Sciences*, 14, 1881-1893,  
717 doi:10.5194/hess-14-1881-2010.

718 Brown, C., R. Meeks, K. Hunu, and W. Yu, 2011: Hydroclimate risk to economic growth  
719 in sub-Saharan Africa. *Climatic Change*, 106, 621–647. DOI 10.1007/s10584-010-  
720 9956-9

721 Camberlin, P., S. Janicot, and I. Pocard, 2001: Seasonality and atmospheric dynamics of  
722 the teleconnection between African rainfall and tropical sea-surface temperature:  
723 Atlantic vs. ENSO. *Int. J. Climatol.*, 21(8), 973-1005, doi: 10.1002/joc.673.

724 Chaney, N. W., and J. Sheffield, 2012: Deriving runoff fields over Africa: Spatial  
725 disaggregation of GRDC stream gauges. GRDC Report Series (Submitted).

726 Chaney, N. W., J. Sheffield, G. Villarini, and E. F. Wood, 2013: Spatial analysis of trends  
727 in climatic extremes with a high resolution gridded daily meteorological data set over  
728 sub-Saharan Africa. In preparation.

729 Crow, W. T., M. J. van den Berg, G. J. Huffman, and T. Pellarin, 2011: Correcting  
730 rainfall using satellite-based surface soil moisture retrievals: The Soil Moisture  
731 Analysis Rainfall Tool (SMART), *Water Resour. Res.*, 47, W08521,  
732 doi:10.1029/2011WR010576

733 De Jeu, R. A. M., W. W. Wagner, T. R. H. Holmes, A. J. Dolman, N. C. van de Giesen,  
734 and J. Friesen, 2008: Global Soil Moisture Patterns Observed by Space Borne  
735 Microwave Radiometers and Scatterometers, *Surveys in Geophysics*, 28, 399-420 doi  
736 10.1007/s10712-008-9044-0.

737 Dixon, J. and A. Gulliver with D. Gibbon, 2001: Farming Systems and Poverty:  
738 Improving Farmers' Livelihoods in a Changing World. FAO & World Bank, Rome,  
739 Italy & Washington, DC, USA.

740 Dutra, E., L. Magnusson, F. Wetterhall, H. L. Cloke, G. Balsamo, S. Boussetta, and F.  
741 Pappenberger, 2012a: The 2010-2011 drought in the Horn of Africa in ECMWF  
742 reanalysis and seasonal forecast products. *Int. J. Climatol.*, doi:10.1002/joc.3545.

743 Dutra, E., F. Di Giuseppe, F. Wetterhall, and F. Pappenberger, 2012b: Seasonal forecasts  
744 of drought indices in African basins. *Hydrol. Earth Syst. Sci. Discuss.*, 9, 11093-  
745 11129, doi:10.5194/hessd-9-11093-2012.

746 Duan, Q., S. Sorooshian, and V. K. Gupta, 1992: Effective and efficient global  
747 optimization for conceptual rainfall-runoff models. *Water Resources Research*, 28,  
748 1015-1031.

749 FAO, 1995: The Digital Soil Map of the World, Version 3.5. United Nations Food and  
750 Agriculture Organization, CD-ROM. [Available from Food and Agriculture  
751 Organization of the United Nations, Viale delle Terme di Caracalla, 00100 Rome,  
752 Italy]

753 FAO/FEWSNET, 2013: Mortality among populations of southern and central Somalia  
754 affected by severe food insecurity and famine during 2010-2012. FAO/FEWSNET  
755 Report, May 2013.

756 Funk, C., and M. Brown, 2005: A maximum to minimum technique for making  
757 projections of NDVI in semi-arid Africa for food security early warning. *Rem. Sens.*  
758 *Env.*, 101, 249-256.

759 Gao, H., C. Birkett, and D. P. Lettenmaier, 2012: Global monitoring of large reservoir  
760 storage from satellite remote sensing, *Water Resour. Res.*, 48, W09504,  
761 doi:10.1029/2012WR012063

762 Gao, H., Q. Tang, C. Ferguson, E.F. Wood, and D. P. Lettenmaier, 2010: Estimating the  
763 water budget of major U.S. river basins via remote sensing. *Int. J. Rem. Sen.*, 31(14),  
764 3955-3978.

765 Guan, K., Wood, E. F. and Caylor, K. K., 2012: Multi-sensor derivation of regional  
766 vegetation fractional cover in Africa. *Rem. Sen. of Env.*, 124, 653-665.

767 Guan, K., Wolf, A., Medvigy, D., Caylor, K., Pan, M. and Wood, E., 2013: Seasonal  
768 coupling of canopy structure and function in African tropical forests and its  
769 environmental controls. *Ecosphere*, 4(3).

770 Guo, Z., and Coauthors, 2006: Evaluation of GSWP-2 soil moisture simulations. Part II:  
771 Sensitivity to external meteorological forcing. *J. Geophys. Res.*, 111.D22S03,  
772 doi:10.1029/2006JD007845.

773 Gobena, A. K., and T. Y. Gan, 2010: Incorporation of seasonal climate forecasts in the  
774 ensemble streamflow prediction system, *J. Hydr.*, 385(1-4), 336-352.

775 Gruhier, C., T. Pellarin, P. de Rosnay, Y. Kerr, 2013: SMOS soil moisture product  
776 evaluation over West-Africa at local and regional scale, under review.

777 Haile, M., 2005: Weather patterns, food security and humanitarian response in sub-  
778 Saharan Africa, *Philosophical Transactions of the Royal Society B-Biological*  
779 *Sciences*, 360(1463), 2169-2182, doi: 10.1098/rstb.2005.1746.

780 Haddeland, I., T. Skaugen, and D.P. Lettenmaier, 2007: Hydrologic effects of land and  
781 water management in North America and Asia: 1700-1992. *Hydrol. Earth Sys. Sci.*,  
782 11(2), 1035-1045.

783 Hansen, M. C., R. S. DeFries, J. R. G. Townshend, and R. Sohlberg, 2000: Global land  
784 cover classification at 1 km spatial resolution using a classification tree approach, *Int.*  
785 *J. Remote Sens.*, 21, 1331–1364.

786 Hansen, J. W., S. Mason, L. Sun, and A. Tall, 2011: Review of seasonal climate  
787 forecasting for agriculture in sub-Saharan Africa. *Expl. Agric.*, 47 (2), 205-240.  
788 doi:10.1017/S0014479710000876.

789 Hayes, M., O. Wilhelmi, and C. Knutson, 2004: Reducing drought risk: Bridging theory  
790 and practice. *Nat. Hazards Rev.* doi:10.1061/(asce)1527-6988(2004)5:2(106)

791 Heim, R. R., and M. J. Brewer, 2012: The Global Drought Monitor Portal: The  
792 Foundation for a Global Drought Information System. *Earth Interact.*, 16, 1–28. doi:  
793 <http://dx.doi.org/10.1175/2012EI000446.1>

794 Henderson-Sellers, A, Z-L Yang, and R.E. Dickinson, 1993: The Project for  
795 Intercomparison of Land-surface Parameterization Schemes, *Bulletin of American*  
796 *Meteorological Society*, 74:1335-1349.

797 Houborg, R., M. Rodell, B. Li, R. Reichle, and B. F. Zaitchik, 2012: Drought indicators  
798 based on model-assimilated Gravity Recovery and Climate Experiment (GRACE)  
799 terrestrial water storage observations. *Water Resources Research*, 48, 7

800 Huffman, G. J., R. F. Adler, D. T. Bolvin, and G. Gu, 2009: Improving the global  
801 precipitation record: GPCP Version 2.1, *Geophys. Res. Lett.*, 36(17), L17808, doi:  
802 10.1029/2009gl040000.

803 Ingram, K. T., M. C. Roncolia, and P. H. Kirshen, 2002: Opportunities and constraints for  
804 farmers of west Africa to use seasonal precipitation forecasts with Burkina Faso as a  
805 case study. *Agricultural Systems*, 74 (3), 331–349.

806 Jarlan, L., E. Mougin, P. Frison, P. Mazzeg, and P. Hiernaux, 2002: Analysis of ERS  
807 wind scatterometer time series over Sahel (Mali). *Remote Sensing of Environment* **81**,  
808 404-415.

809 Jin, E., and Coauthors, 2008: Current status of ENSO prediction skill in coupled ocean-  
810 atmosphere models. *Climate Dyn.*, 31(6), 647-664, doi: 10.1007/s00382-008-0397-3.

811 Jones, L. A., and Kimball, J. S., 2012: A global daily record of land parameter retrievals  
812 from AMSR-E (Version 1.2, Update 1), Numerical Terradynamic Simulation Group  
813 (NTSG), The University of Montana.

814 Jones, M. O., J. S. Kimball, L. Jones, and K. C. McDonald, 2012: Satellite passive  
815 microwave detection of North America start of season. *Remote Sensing of*  
816 *Environment*, 123, 324-333.

817 Kerr Y., P. Waldteufel, P. Richaume, J.-P. Wigneron, P. Ferrazzoli, A. Mahmoodi, A. Al  
818 Bitar, F. Cabot, C. Gruhier, S. Juglea, D. Leroux, A. Mialon, and S. Delwart, 2012:  
819 The SMOS Soil Moisture Retrieval Algorithm. *IEEE TGRS*, 50(5), 1384-1403. DOI:  
820 10.1109/TGRS.2012.2184548.

821 Kotir, J., 2011: Climate change and variability in Sub-Saharan Africa: a review of current  
822 and future trends and impacts on agriculture and food security. *Environment,*  
823 *Development and Sustainability*, 13 (3), 587-605.

824 Lavers, D., L. Luo, and E. F. Wood, 2009: A multiple model assessment of seasonal  
825 climate forecast skill for applications, *Geophys. Res. Lett.*, 36(23), L23711

826 Li, H., L. Luo, E. F. Wood, and J. Schaake, 2009: The role of initial conditions and  
827 forcing uncertainties in seasonal hydrologic forecasting, *J. Geophys. Res.*, 114,  
828 D04114, doi:10.1029/2008JD010969.

829 Liang, X., E. F. Wood, and D. P. Lettenmaier, 1996: Surface soil moisture  
830 parameterization of the VIC-2L Evaluation and modification. *Global and Planetary*  
831 *Change*, 13, 195-206.

832 Liu, Y. Y., R. A. M. de Jeu, M. F. McCabe, J. P. Evans, and A. I. J. M. van Dijk, 2011:  
833 Global long- term passive microwave satellite- based retrievals of vegetation optical  
834 depth, *Geophys. Res. Lett.*, 38, L18402, doi:10.1029/2011GL048684.

835 Luo, L., E. F. Wood, and M. Pan, 2007: Bayesian merging of multiple climate model  
836 forecasts for seasonal hydrological predictions, *J. Geophys. Res.*, 112, D10102,  
837 doi:10.1029/2006JD007655.

838 Luo, L., and E. F. Wood, 2008: Use of Bayesian merging techniques in a multi-model  
839 seasonal hydrologic ensemble prediction system for the Eastern U.S. *J. Hydrometeo.*,  
840 5, 866-884.

841 Luseno, W. K., J. G. McPeak, C. B. Barrett, P. D. Little, and G. Gebru, 2003: Assessing  
842 the Value of Climate Forecast Information for Pastoralists: Evidence from Southern  
843 Ethiopia and Northern Kenya. *World Development*, 31 (9), 1477-1494.

844 Lyon, B., and D. G. DeWitt, 2012: A recent and abrupt decline in the East African long  
845 rains. *Geophys. Res. Lett.*, 39, L02702, doi:10.1029/2011GL050337.

846 MacDonald, A. M., H. C. Bonsor, B. É. Ó. Dochartaigh, and R. G. Taylor, 2012:  
847 Quantitative maps of groundwater resources in Africa. *Environ. Res. Lett.*, 7, 024009.  
848 doi:10.1088/1748-9326/7/2/024009.

849 Manatsa, D. L. Unganai, C. Gadzirai, and, S. K. Behera, 2012: An innovative tailored  
850 seasonal rainfall forecasting production in Zimbabwe. *Nat. Hazards*, 64 (2), 1187-  
851 1207. DOI: 10.1007/s11069-012-0286-2.

852 Maxwell, D., and M. Fitzpatrick, 2012: The 2011 Somalia famine: Context, causes, and  
853 complications. *Global Food Security*, 1 (1), 5-12.

854 Mckee, T. B., N. J. Doesken, and J. Kleist, 1993: The relationship of drought frequency  
855 and duration to time scales. Eighth Conference on Applied Climatology.

856 Milzow, C., P. E. Krogh, and P. Bauer-Gottwein, 2010: Combining satellite radar  
857 altimetry, SAR surface soil moisture and GRACE total storage changes for model

858 calibration and validation in a large ungauged catchment. *Hydrology and Earth*  
859 *System Sciences Discussions*, 7 (6), 9123-9154.

860 Mitchell, K. E., D. Lohmann, P. R. Houser, E. F. Wood, J. C. Schaake, A. Robock, B. A.  
861 Cosgrove, J. Sheffield, Q. Duan, L. Luo, R. W. Higgins, R. T. Pinker, J. D. Tarpley,  
862 D. P. Lettenmaier, C. H. Marshall, J. K. Entin, M. Pan, W. Shi, V. Koren, J. Meng, B.  
863 H. Ramsay, and A. A. Bailey, 2004: The Multi-institution North American Land Data  
864 Assimilation System (NLDAS): Utilizing multiple GCIP products and partners in a  
865 continental distributed hydrological modeling system. *J. Geophys. Res.*, 109, D07S90,  
866 doi: 10.1029/2003JD003823.

867 Mortimore, M. J., and W. M. Adams, 2001: Farmer adaptation, change and ‘crisis’ in the  
868 Sahel. *Global Environmental Change*, 11, 49–57.

869 Mu, Q., F. A. Heinsch, M. Zhao, S. W. Running, 2007: Development of a global  
870 evapotranspiration algorithm based on MODIS and global meteorology data. *Remote*  
871 *Sensing of Environment*, 111, 519-536. doi: 10.1016/j.rse.2007.04.015.

872 Mu, Q., M. Zhao, J. S. Kimball, N. G. McDowell, and S. W. Running, 2013: A remotely  
873 sensed global terrestrial drought severity index. *Bull. Amer. Meteor. Soc.*, 94, 83–98.  
874 doi: <http://dx.doi.org/10.1175/BAMS-D-11-00213.1>

875 Nash, J. E. and J. V. Sutcliffe, 1970: River flow forecasting through conceptual models  
876 part I - A discussion of principles. *J. Hydrology*, 10 (3), 282–290.

877 NCDC, 2012: Billion-Dollar Weather/Climate Events. Available online:  
878 <http://www.ncdc.noaa.gov/billions>

879 Oettli, P., B. Sultan, C. Baron and M. Vrac, 2011: Are regional climate models relevant  
880 for crop yield prediction in West Africa ? *Environ. Res. Lett.*, 6, 9pp.

881 Ogallo, L., P. Bessemoulin, J. P. Ceron, S. Mason, S., and S. J. Connor, 2008: Adapting  
882 to climate variability and change: The climate outlook forum process. *WMO Bulletin*,  
883 57, 93–102.

884 Pan, M., H. Li, and E. F. Wood. 2010: Assessing the Skill of Satellite-based Precipitation  
885 Estimates in Hydrologic Applications, *Water Resources Research*, 46, W09535,  
886 doi:10.1029/2009WR008290.

887 Pan, M., A. K. Sahoo, T. J. Troy, R. K. Vinukollu, J. Sheffield, and E. F. Wood, 2012:  
888 Multisource estimation of long-term terrestrial water budget for major global river  
889 basins. *J. Climate*, 25 (9), 3191-3206. DOI: 10.1175/JCLI-D-11-00300.1.

890 Pan, M., A. K. Sahoo, E. F. Wood, A. Al-Bitar, D. Leroux, and Y. Kerr, 2012: An Initial  
891 Assessment of SMOS derived Soil Moisture over the Continental United States, *IEEE*  
892 *Journal of Selected Topics in Applied Earth Observations and Remote Sensing*,  
893 doi:10.1109/JSTARS.2012.2194477 (in press).

894 Pappenberger, F., J. Thielen, and M. Del Medico, 2011: The impact of weather forecast  
895 improvements on large scale hydrology: analysing a decade of forecasts of the  
896 European Flood Alert System. *Hydr. Proc.*, 25(7), 1091-1113.

897 Patt, A. G., L. Ogallo, and M. Hellmuth, 2007: Learning from 10 years of Climate  
898 Outlook Forums in Africa. *Science*, 318 (5847), 49-50. DOI:  
899 10.1126/science.1147909.

900 Pellarin, T., A. Ali, F. Chopin, I. Jobard, J.-C. Bergès, 2008: Using spaceborne surface  
901 soil moisture to constrain satellite precipitation estimates over West Africa.  
902 *Geophysical Research Letters*, 35, L02813, doi:10.1029/2007GL032243.

903 Pellarin, T., S. Louvet, C. Gruhier, G. Quantin, and C. Legout, 2012: A simple and  
904 effective method for correcting soil moisture and precipitation estimates using  
905 AMSR-E measurements, *Remote Sensing of Environment*, submitted.

906 Pozzi, W., J. Sheffield, R. Stefanski, D. Cripe, R. Pulwarty, et al., 2013: Framework for  
907 global drought early warning: Expanding international cooperation for development  
908 of a framework for global drought monitoring and forecasting. *Bull. Amer. Meteor.*  
909 *Soc.*, in press.

910 Quan, X.-W., M. Hoerling, B. Lyon, A. Kumar, M. Bell, M. Tippett, and H. Wang, 2012:  
911 Prospects for dynamical prediction of meteorological drought. *J. Appl. Meteor.*  
912 *Climatol.*, 51, 1238-1252.

913 Roncoli, C., 2006: Ethnographic and participatory approaches to research on farmers'  
914 responses to climate predictions. *Clim. Res.*, 33, 81-99.

915 Roncoli, C., B. S. Orlove, M. R. Kabugo, and M. M. Waiswa, 2011: Cultural styles of  
916 participation in farmers' discussions of seasonal climate forecasts in Uganda.  
917 *Agriculture and Human Values*, 28 (1), 123-138.

918 Rowell, D. P., 2013: Simulating SST Teleconnections to Africa: What is the State of the  
919 Art? *J. Climate*, doi: <http://dx.doi.org/10.1175/JCLI-D-12-00761.1>

920 Saha, S., and Coauthors, 2006: The NCEP Climate Forecast System. *J. Climate*, 19,  
921 3483–3517. doi: <http://dx.doi.org/10.1175/JCLI3812.1>

922 Sahoo, A. K., G. D. L. De Lannoy, R. Reichle, and P. Houser, 2012: Assimilation and  
923 Downscaling of Satellite Observed Soil Moisture over the Little River Experimental  
924 Watershed in Georgia, USA. *Advances in Water Resources*, (in press).

925 Sahoo, A., E. F. Wood, J. Sheffield, M. Pa, A. Albitar, D. Leroux, and Y. Kerr, 2011: A  
926 strategy for global drought monitoring using SMOS soil moisture observations.  
927 *Geophysical Research Abstracts*, Vol. 13, EGU2011-8409.

928 Sellers, P. J., J. A. Berry, G. J. Collatz, C. B. Field, and E. G. Hall, 1992: Canopy  
929 Reflectance, Photosynthesis, and Transpiration. III. A Reanalysis Using Improved  
930 Leaf Models and a New Canopy Integration Scheme. *Remote Sensing of Environment*  
931 42, 187-216.

932 Seneviratne, S. I., N. Nicholls, D. Easterling, C. M. Goodess, S. Kanae, J. Kossin, Y.  
933 Luo, J. Marengo, K. McInnes, M. Rahimi, M. Reichstein, A. Sorteberg, C. Vera, and  
934 X. Zhang, 2012: Changes in climate extremes and their impacts on the natural  
935 physical environment. In: *Managing the Risks of Extreme Events and Disasters to*  
936 *Advance Climate Change Adaptation* [Field, C.B., V. Barros, T.F. Stocker, D. Qin,  
937 D.J. Dokken, K.L. Ebi, M.D. Mastrandrea, K.J. Mach, G.-K. Plattner, S.K. Allen, M.  
938 Tignor, and P.M. Midgley (eds.)]. A Special Report of Working Groups I and II of  
939 the Intergovernmental Panel on Climate Change (IPCC). Cambridge University Press,  
940 Cambridge, UK, and New York, NY, USA, pp. 109-230.

941 Sheffield, J., G. Goteti, F. Wen, and E. F. Wood, 2004: A simulated soil moisture based  
942 drought analysis for the United States, *J. Geophys. Res.*, 109, D24108,  
943 doi:10.1029/2004JD005182.

944 Sheffield, J., G. Goteti, and E. F. Wood, 2006: Development of a 50-yr high-resolution  
945 global dataset of meteorological forcings for land surface modeling, *J. Climate*, 19  
946 (13), 3088-3111.

947 Sheffield J., and E. F. Wood, 2008: Projected changes in drought occurrence under future  
948 global warming from multi-model, multi-scenario, IPCC AR4 simulations, *Climate*  
949 *Dynamics*, 13 (1), 79-105, doi:10.1007/s00382-007-0340-z.

950 Sheffield, J., K. M. Andreadis, E. F. Wood, and D. P. Lettenmaier, 2009: Global and  
951 continental drought in the second half of the 20th century: severity-area-duration  
952 analysis and temporal variability of large-scale events, *J. Climate*, 22(8), 1962-1981.

953 Sheffield, J., and E. F. Wood, 2011: Drought: Past Problems and Future Scenarios,  
954 Earthscan, UK, pp 192.

955 Shukla, S., J. Sheffield, E. F. Wood, and D. P. Lettenmaier, 2013: On the sources of  
956 global land surface hydrologic predictability, *Hydrol. Earth Syst. Sci. Discuss.*, 10,  
957 1987-2013, doi:10.5194/hessd-10-1987-2013.

958 Smith, D. M., A. A. Scaife, and B. P. Kirtman, 2012: What is the current state of  
959 scientific knowledge with regard to seasonal to decadal forecasting. *Environ. Res.*  
960 *Lett.*, 7, 015602.

961 Stisen, S., and I. Sandholt, 2010: Evaluation of remote-sensing-based rainfall products  
962 through predictive capability in hydrological runoff modelling. *Hydrol. Process.*, 24,  
963 879–891.

964 Svoboda, M., and Coauthors, 2002: The Drought Monitor. *Bull. Amer. Meteor. Soc.*,  
965 83(8), 1181-1190, doi: 10.1175/1520-0477(2002)083<1181:tdm>2.3.co;2.

966 Sylla, M. B., F. Giorgi, E. Coppola, and L. Mariotti, 2012: Uncertainties in daily rainfall  
967 over Africa: assessment of gridded observation products and evaluation of a regional  
968 climate model simulation. *Int. J. Climatol.*. doi: 10.1002/joc.3551

969 Tallaksen, L. M., and H. A. J. van Lanen (eds) *Hydrological Drought: Processes and*  
970 *Estimation Methods for Streamflow and Groundwater*, Developments in Water  
971 Science, Elsevier Science B.V., vol 48, pp53–96

972 Tang, Q., H. Gao, H. Lu, and D. P. Lettenmaier, 2009: Remote sensing: hydrology.  
973 *Progress in Physical Geography*, 33, 490. DOI: 10.1177/0309133309346650.

974 Tapley, B. D., S. Bettadpur, J. C. Ries, P. F. Thompson, and M. M. Watkins, 2004:  
975 GRACE Measurements of Mass Variability in the Earth System, *Science*, 305(5683),  
976 503-505.

977 Tarhule, A., and P. J. Lamb, 2003: Climate research and seasonal forecasting for West  
978 Africans: perceptions, dissemination, and use? *Bull. Amer. Met. Soc.*, 84, 1741–1759.

979 Troy, T. J., E. F. Wood, and J. Sheffield, 2008: An efficient calibration method for  
980 continental-scale land surface modeling. *Water Resources Research*, 44.

981 Tucker, C. J., J. E. Pinzon, M. E. Brown, D. A. Slayback, E. W. Paka, E. Mahoney, E. F.  
982 Vermote, and N. E. Saleous, 2005: An extended AVHRR 8-km NDVI dataset  
983 compatible with MODIS and SPOT vegetation NDVI data. *International Journal of*  
984 *Remote Sensing*, 26 (20), 4485-4498.

985 UN Millennium Project, 2005: Investing in development: a practical plan to achieve the  
986 millennium development goals (ed. J. D. Sachs). London: Earthscan Publications.

987 UN/ISDR, 2007: Drought risk reduction framework and practices: Contributing to the  
988 implementation of the Hyogo Framework for Action, United Nations Secretariat of  
989 the International Strategy for Disaster Reduction, Geneva, Switzerland.

990 UNOCHR, United Nations Organization for the Coordination of Humanitarian Affairs,  
991 2011: Eastern Africa Drought Humanitarian Report 4, 15 July, New York, NY.

992 van Dijk, A. I. J. M., and L. J. Renzullo, 2011: Water resource monitoring systems and  
993 the role of satellite observations. *Hydrology and Earth System Sciences*, 15 (1), 39-  
994 55.

995 van Dijk, A., J. Peña-Arancibia, E. F. Wood, J. Sheffield, H. Beck, 2013: Seasonal  
996 streamflow predictability: skill of a global ensemble streamflow prediction system  
997 assessed for 6192 small catchments worldwide, *Water. Resour. Res.*, accepted

998 Vinukollu, R. K., R. Meynadier, J. Sheffield, and E. F. Wood, 2011: Multi-model, multi-  
999 sensor estimates of global evapotranspiration: climatology, uncertainties and trends.  
1000 *Hydrol. Process.*, 25: 3993–4010. doi: 10.1002/hyp.8393.

1001 Wang, A., D. P. Lettenmaier, and J. Sheffield, 2011: Soil moisture drought in China,  
1002 1950-2006. *J Climate*, 24 (13), 3257-3271. doi: 10.1176/2011JCLI3733.1

1003 Wardlow, B., M. Anderson and J. Verdin (eds.), 2012: Remote sensing of drought:  
1004 Innovative monitoring approaches. Taylor and Francis, London, United Kingdom, p.  
1005 270.

1006 Webster P. J., and J. Jian 2011: Probability, uncertainty and prediction: A pathway  
1007 towards the alleviation of poverty in the developing world. *Phil. Trans. Roy. Soc.*,  
1008 369 (1956).

1009 Webster, P. J., 2013: Improve weather forecasts for the developing world. *Nature*, 493,  
1010 17. doi: 10.1038/493017a.

1011 Weisheimer, A., F. J. Doblas-Reyes, T. N. Palmer, A. Alessandri, A. Arribas, M. Déqué,  
1012 N. Keenlyside, M. MacVean, A. Navarra, and P. Rogel, 2009: ENSEMBLES: A new  
1013 multi-model ensemble for seasonal-to-annual predictions-Skill and progress beyond

1014 DEMETER in forecasting tropical Pacific SSTs. *Geophys. Res. Lett.*, 36, L21711,  
1015 doi:10.1029/2009GL040896.

1016 Williams, A. P, and C. Funk, 2011: A westward extension of the warm pool leads to a  
1017 westward extension of the Walker circulation, drying eastern Africa. *Climate*  
1018 *Dynamics*, 37 (11-12), 2417-2435. DOI: 10.1007/s00382-010-0984-y.

1019 Vogt, J. V., P. Barbosa, B. Hofer, and A. Singleton, 2011: Developing a European  
1020 Drought Observatory for Monitoring, Assessing and Forecasting Droughts across the  
1021 European Continent, *Geophysical Research Abstracts*, European Geosciences Union,  
1022 13.

1023 Xia, Y., K. Mitchell, M. Ek, J. Sheffield, B. Cosgrove, E. Wood, L. Luo, C. Alonge, H.  
1024 Wei, J. Meng, B. Livneh, D. Lettenmaier, V. Koren, Q. Duan, K. Mo, Y. Fan, D.  
1025 Mocko, 2012: Continental-Scale Water and Energy Flux Analysis and Validation for  
1026 the North-American Land Data Assimilation System Project Phase 2 (NLDAS-2),  
1027 Part 1: Intercomparison and Application of Model Products. *J. Geophys. Res.*, Vol.  
1028 117, No. D3, D03110, <http://dx.doi.org/10.1029/2011JD016051>

1029 Yilmaz, K. K., Adler, R.F., Tian, Y., Hong, Y., Pierce, H., 2010: Evaluation of a  
1030 Satellite-based Global Flood Monitoring System. *International Journal of Remote*  
1031 *Sensing*, 31(14), 3763-3782. doi: 10.1080/01431161.2010.483489

1032 Yoon, J. H., K. Mo, and E. F. Wood, 2012: Dynamic-model-based seasonal prediction of  
1033 meteorological drought over the contiguous United States. *J. Hydrometeor.*, 13, 463-  
1034 481.

1035 Yuan, X., E. F. Wood, L. Luo, and M. Pan, 2011: A first look at Climate Forecast System  
1036 version 2 (CFSv2) for hydrological seasonal prediction. *Geophys. Res. Lett.*, 38,  
1037 L13402. doi:10.1029/2011GL047792.

1038 Yuan, X., E. F. Wood, N. W. Chaney, J. Sheffield, J. Kam, M. Liang, and K. Guan, 2013:  
1039 Probabilistic seasonal forecasting of African drought by dynamical models. *J.*  
1040 *Hydrometeor.*, in review.

1041 Yuan, X., and E. F. Wood, 2013: Multi-model seasonal forecasting of global drought  
1042 onset. *Geophys. Res. Lett.*, doi:10.1002/grl.50949, in press.

1043 Zhou, T., B. Nijssen, G. J. Huffman, and D. P. Lettenmaier, 2013: Evaluation of the  
1044 TRMM real-time multi-satellite precipitation analysis version 7 for macro scale  
1045 hydrologic prediction. *Geophysical Research Letters* (submitted)

1046 Ziervogel, G., and R. Calder, 2003: Climate variability and rural livelihoods: assessing  
1047 the impact of seasonal climate forecasts in Lesotho. *Area*, 35(4), 403-417.

1048 Ziervogel, G., P. Johnston, M. Matthew, and P. Mukheibir, 2010: Using climate  
1049 information for supporting climate change adaptation in water resource management  
1050 in South Africa. *Climatic Change*, 103. 3-4. 537-554.

1051

1052

1053

1054

1056 **Table 1.** Drought indices represented in the African Drought Monitor and their attributes.

Index	Data Source	Drought Type	Attributes
Standardized Precipitation Index (SPI)	Bias corrected TMPA (2009-present), hybrid observational/reanalysis (1950-2008)	Meteorological drought	0.25-degree, SPI-1,3,6,12
VIC Soil Moisture Index	VIC land surface model (1950-present);	Agricultural drought	0.25-degree, daily
SMOS Soil Moisture Index	SMOS retrievals (2010-present)	Agricultural drought (top 5cm of soil)	0.25-degree, daily
NDVI/EVI	GIMMS NDVI (1982-2008); MODIS EVI (2000-present);	Ecological drought (optical-based)	8km/0.5-degree, bi-monthly/daily
VOD Index	SSM/I, TRMM, AMSR-E VOD (1987-2008); AMSR-E VOD (2000-present)	Ecological drought (passive microwave)	0.25-degree, daily
dB Index	QuickSCAT (1999-2009), ASCAT (2009-present)	Ecological-hydrological drought (active microwave)	0.25-degree, 2/4 days

Streamflow percentiles	VIC land surface model (1950-present)	Hydrological drought	822 streamflow gauges, daily/monthly
Cumulative streamflow deficit	VIC land surface model (1950-present)	Hydrological drought	822 streamflow gauges, daily/monthly

1057

1058

1059 **Figure Captions**

1060 **Figure 1.** Seasonal mean precipitation for 1950-2008 for (a) December-February, (b)  
1061 March-May, (c) June-August and (d) September-November.

1062 **Figure 2.** Seasonal standard deviation of precipitation for 1950-2008 for (a) December-  
1063 February, (b) March-May, (c) June-August and (d) September-November.

1064 **Figure 3.** Flow chart of the African Drought Monitor and Forecast System. The system  
1065 comprises three parts: 1) Historic reconstructions of the terrestrial hydrological cycle that  
1066 is derived from simulations of the VIC land surface model forced by a hybrid reanalysis-  
1067 observational meteorological dataset. The datasets are used for a variety of applications  
1068 including analysis of historic drought events, estimation of trends and variability, and  
1069 investigation of drought mechanisms. 2) Real-time monitoring component that updates  
1070 the model run to 2-3 days from real-time forced by bias-corrected and downscaled TMPA  
1071 satellite precipitation and GFS analysis fields of temperature and windspeed. There is  
1072 also potential to force other impact models such as crop models. 3) Seasonal hydrological  
1073 forecast component that uses bias-corrected and downscaled CFSv2 climate forecasts of  
1074 precipitation and temperature to drive the model and provide ensemble predictions of  
1075 drought conditions, for precipitation, soil moisture and streamflow. Existing components  
1076 are shown in normal font, and potential future components in italic font.

1077 **Figure 4.** The African Drought Monitor web interface  
1078 (<http://hydrology.princeton.edu/adm>) enables users to access the system's input and  
1079 output data interactively. Google Maps is used to display the spatial information in an  
1080 efficient and intuitive manner. The user can visualize and animate the temporal evolution  
1081 of the drought-related hydrologic variables over the continent (top right) and select

1082 among the stream gauges monitored in the system to display the time series of the  
1083 evolution of basin averaged water balance variables and drought products (bottom). The  
1084 user can also readily download the data.

1085 **Figure 5.** (a) A training session at the first workshop in January 2012 at the  
1086 AGRHYMET center in Niamey, Niger, in which participants from national  
1087 meteorological and hydrological agencies and river basin management authorities were  
1088 trained in the use of the system. (b) Participants from the second workshop in June 2012  
1089 at the ICPAC center in Nairobi, Kenya.

1090 **Figure 6.** Evaluation of VIC model input and output data. Annual mean precipitation  
1091 (mm/day) for 2003-2008 for (a) the TMPA 3B42RT V6 satellite product, (b) the long-  
1092 term (1948-2008) historic ADM data, (c) and their difference (TMPA - ADM). Monthly  
1093 Nash-Sutcliffe efficiency values of the VIC simulated streamflow with respect to  
1094 available historic GRDC observations for (d) the uncalibrated model, (e) the calibrated  
1095 model, and (f) their difference (calibrated – uncalibrated). Annual mean  
1096 evapotranspiration (mm/day) for 1997-2006 for (g) the RS-PM satellite product of  
1097 Vinokullo et al., (2012), (h) VIC, and (i) their difference (VIC – RS-PM). The seasonal  
1098 range in water storage ( $\Delta S$ ; mm) for 2003-2011 for (j) GRACE JPL rel5, (k) VIC, and (l)  
1099 their difference GRACE - VIC.

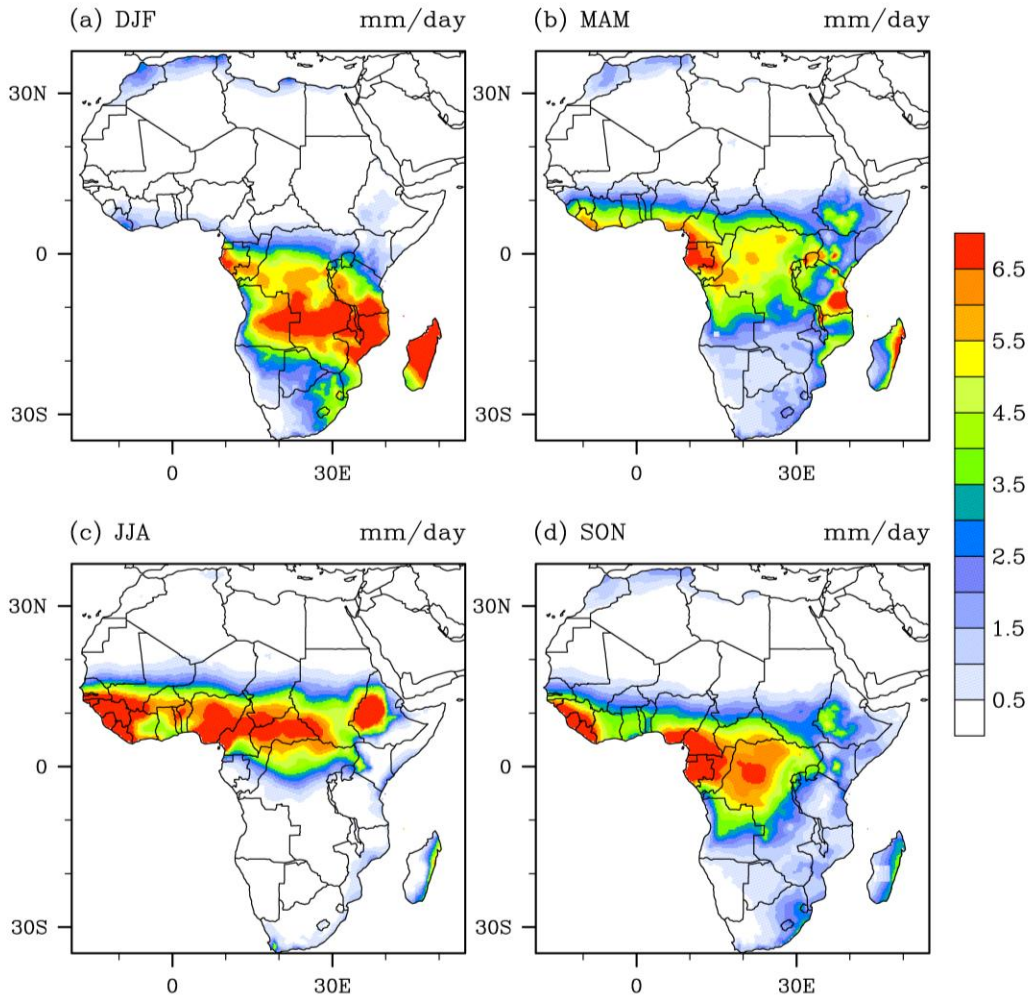
1100 **Figure 7.** An example of streamflow validation over the Greater Horn of Africa region  
1101 for a diverse set of basins. (top right) location of validation sites selected by participants  
1102 from national hydrological agencies at the ICPAC workshop in 2012. (top two rows)  
1103 Examples of time series of simulated streamflow discharge from the ADM compared to  
1104 available observations. The Beledweyne site is on the Shebeelle River in south-central

1105 Somalia, which is an area of intensive irrigation. The Bardera site is on the Juba River in  
1106 southern Somalia, which is an important agricultural area. Note the lack of observational  
1107 data during the peak of the Somali civil war in the 1990s. The Ndago site is in a small  
1108 catchment in southwestern Burundi. The Ruizi site is in southwestern Uganda and may be  
1109 subject to water abstractions. The Kapiri site in eastern Uganda is in a wetland area  
1110 between two lakes. (bottom row) Summary comparisons for 16 sites in Somalia, Uganda  
1111 and Burundi for (left) mean flows, (middle) 3-day peak flows, and (bottom) 7-day low  
1112 flows. The median (horizontal line), inter-quartile range (box) and range (whiskers) are  
1113 shown for the observations and ADM predictions.

1114 **Figure 8.** Brier skill score for 1, 2 and 3-month forecasts of soil moisture for (a) West  
1115 Africa (forecast date = 15 April), (b) East Africa (forecast date = 15 March) and (c)  
1116 Southern Africa (forecast date = 15 October). The forecasts are from VIC model  
1117 simulated soil moisture forced by bias-corrected and downscaled CFSv2 climate  
1118 forecasts, and evaluated relative to the VIC observation-forced historic simulation. The  
1119 reference forecast is the soil moisture climatology from the offline simulation.

1120 **Figure 9.** The evolution of the 2010-2011 drought over the Horn of Africa. (left) Time  
1121 series of drought indices averaged over the HoA region (30-52E, 5S-15N) and (right)  
1122 maps of drought indices at the height of the drought as indicated by the gray shading in  
1123 the time series. The bottom time series shows the simulated streamflow at the Agfoi  
1124 gauging station on the Shebelle River (upstream area = 107,336 km<sup>2</sup>), which flows from  
1125 the Ethiopian highlands and is one of the two main rivers (along with the Jubba River) in  
1126 southern Somalia. All indices except SPI3 are calculated as percentiles.

1127 **Figure 10.** Seasonal hydrological forecasts of the 2010/11 Horn of Africa drought. (a)  
1128 Soil moisture percentile averaged over the main drought region (40-52E, 3-12N) from the  
1129 historic VIC simulation, September 2010 forecast and February 2011 forecast. (b)  
1130 Percent area in drought based on a drought threshold of the 20th percentile of soil  
1131 moisture for the historic simulation and the two forecasts. The forecasts are shown for 10  
1132 ensemble members and the ensemble mean (thick lines).  
1133



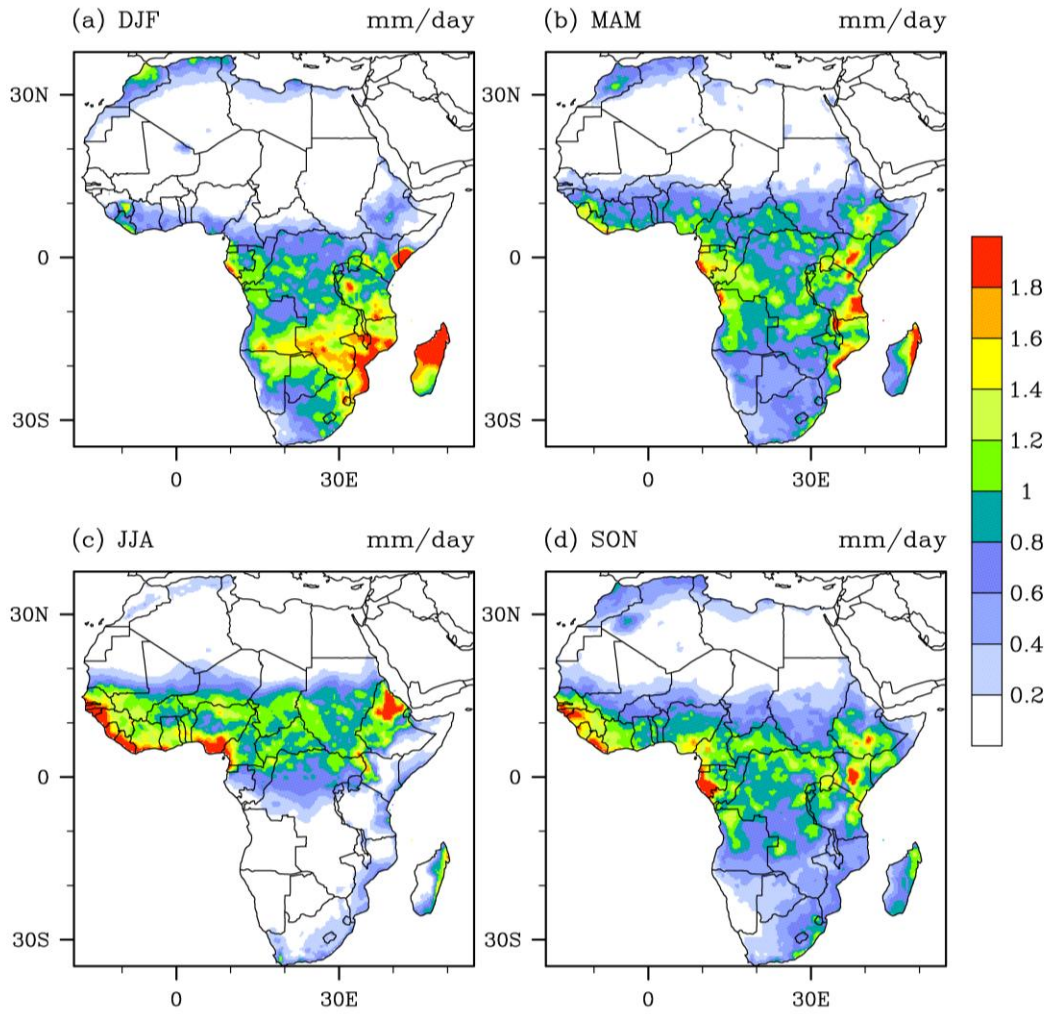
1135

1136

1137 **Figure 1.** Seasonal mean precipitation for 1950-2008 for (a) December-February, (b)

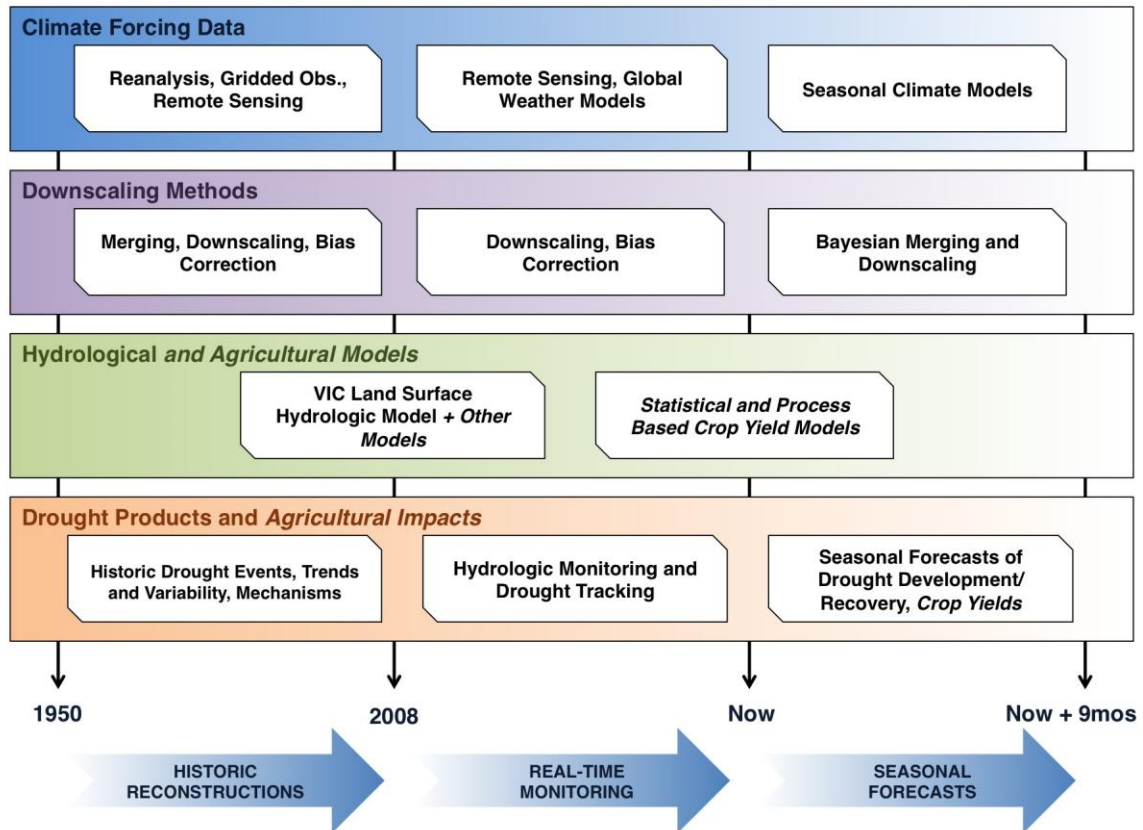
1138 March-May, (c) June-August and (d) September-November.

1139



1140

1141 **Figure 2.** Seasonal standard deviation of precipitation for 1950-2008 for (a) December-  
 1142 February, (b) March-May, (c) June-August and (d) September-November.



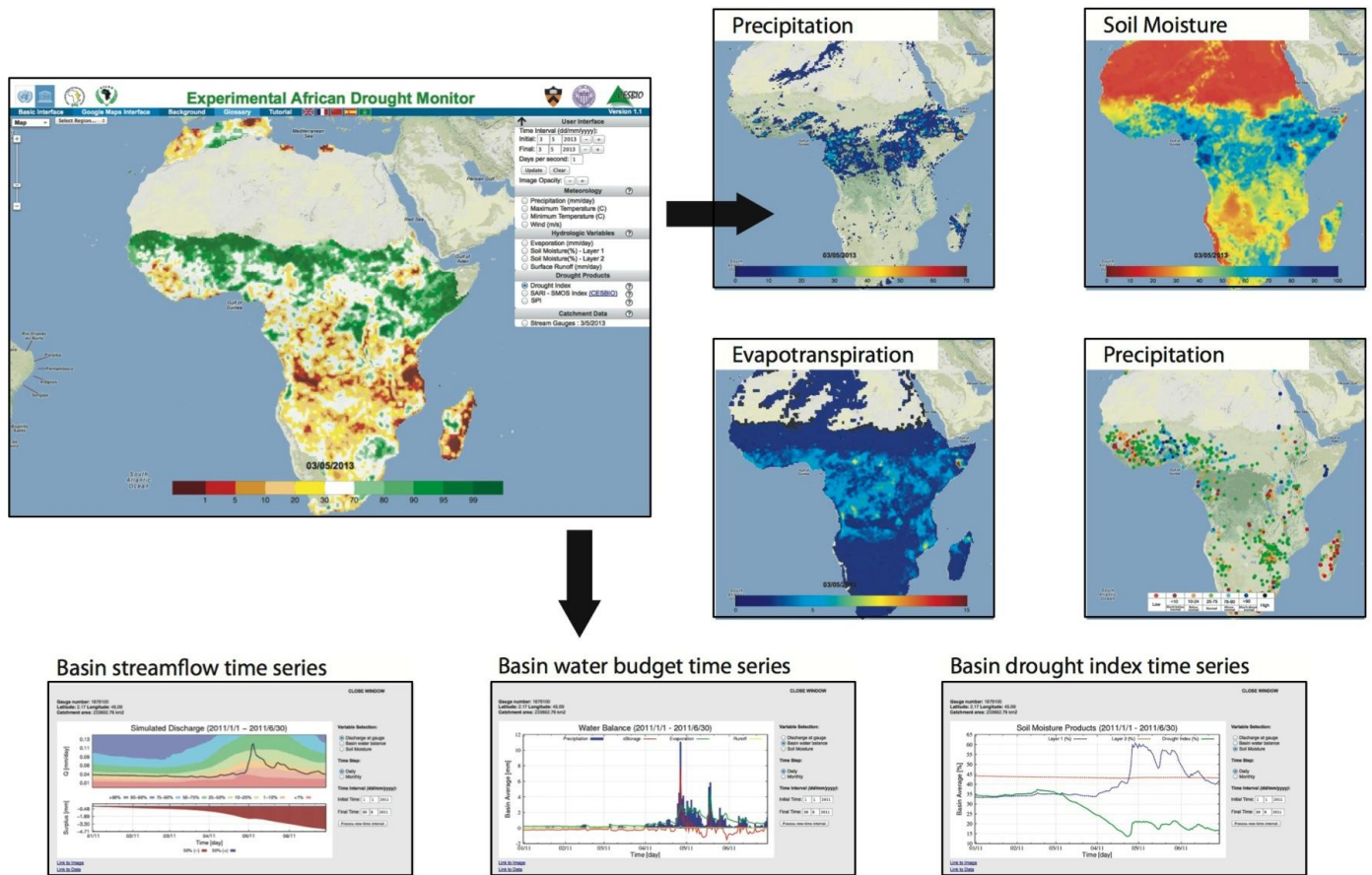
1143

1144 **Figure 3.** Flow chart of the African Drought Monitor and Forecast System. The system  
 1145 comprises three parts: 1) Historic reconstructions of the terrestrial hydrological cycle that  
 1146 is derived from simulations of the VIC land surface model forced by a hybrid reanalysis-  
 1147 observational meteorological dataset. The datasets are used for a variety of applications  
 1148 including analysis of historic drought events, estimation of trends and variability, and  
 1149 investigation of drought mechanisms. 2) Real-time monitoring component that updates  
 1150 the model run to 2-3 days from real-time forced by bias-corrected and downscaled TMPA  
 1151 satellite precipitation and GFS analysis fields of temperature and windspeed. There is  
 1152 also potential to force other impact models such as crop models. 3) Seasonal hydrological  
 1153 forecast component that uses bias-corrected and downscaled CFSv2 climate forecasts of  
 1154 precipitation and temperature to drive the model and provide ensemble predictions of

1155 drought conditions, for precipitation, soil moisture and streamflow. Existing components  
1156 are shown in normal font, and potential future components in italic font.

1157

1158



1160

1161 **Figure 4.** The African Drought Monitor web interface

1162 (<http://hydrology.princeton.edu/adm>) enables users to access the system’s input and

1163 output data interactively. Google Maps is used to display the spatial information in an

1164 efficient and intuitive manner. The user can visualize and animate the temporal evolution

1165 of the drought-related hydrologic variables over the continent (top right) and select

1166 among the stream gauges monitored in the system to display the time series of the

1167 evolution of basin averaged water balance variables and drought products (bottom). The

1168 user can also readily download the data.

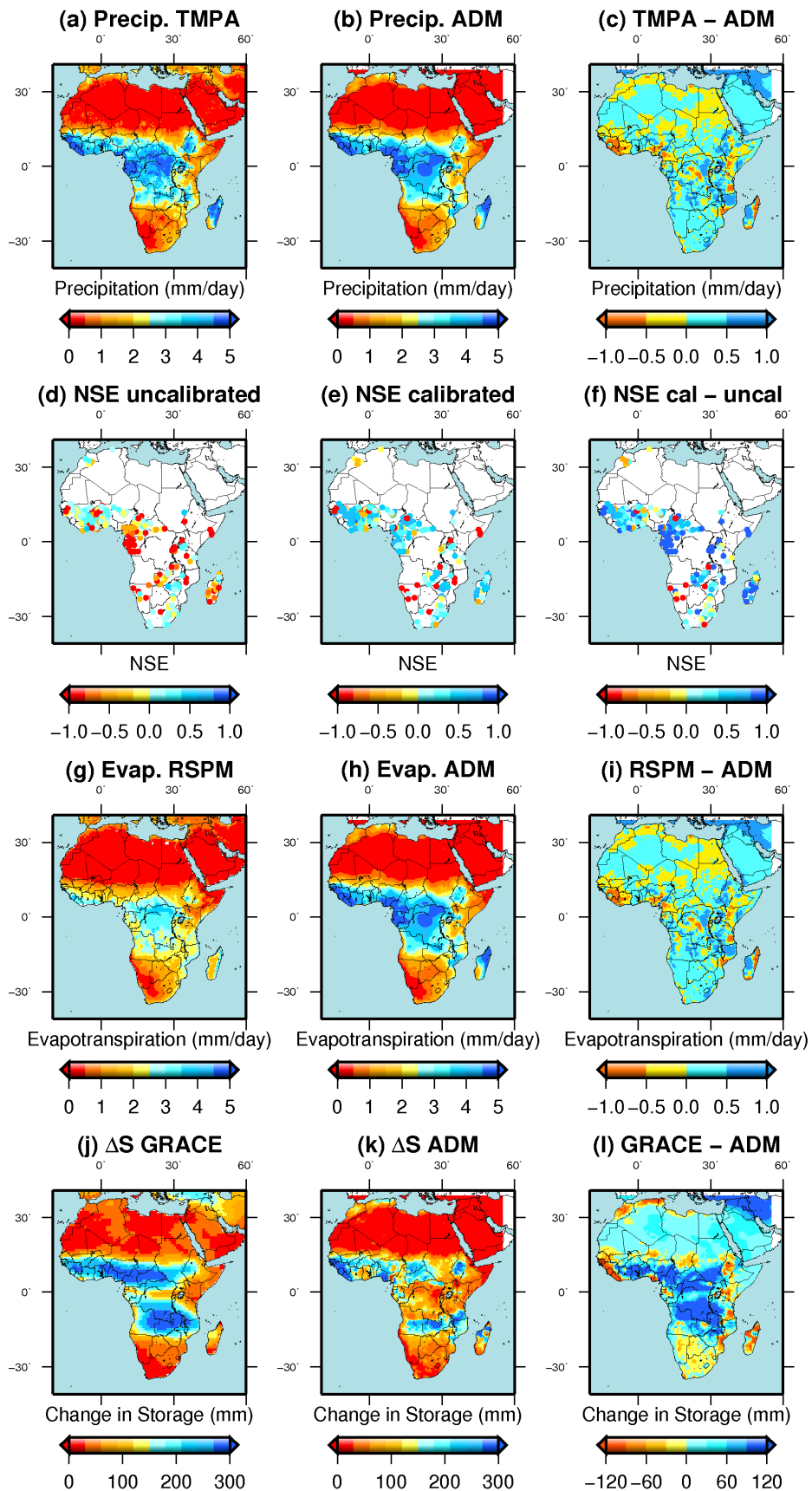


1169

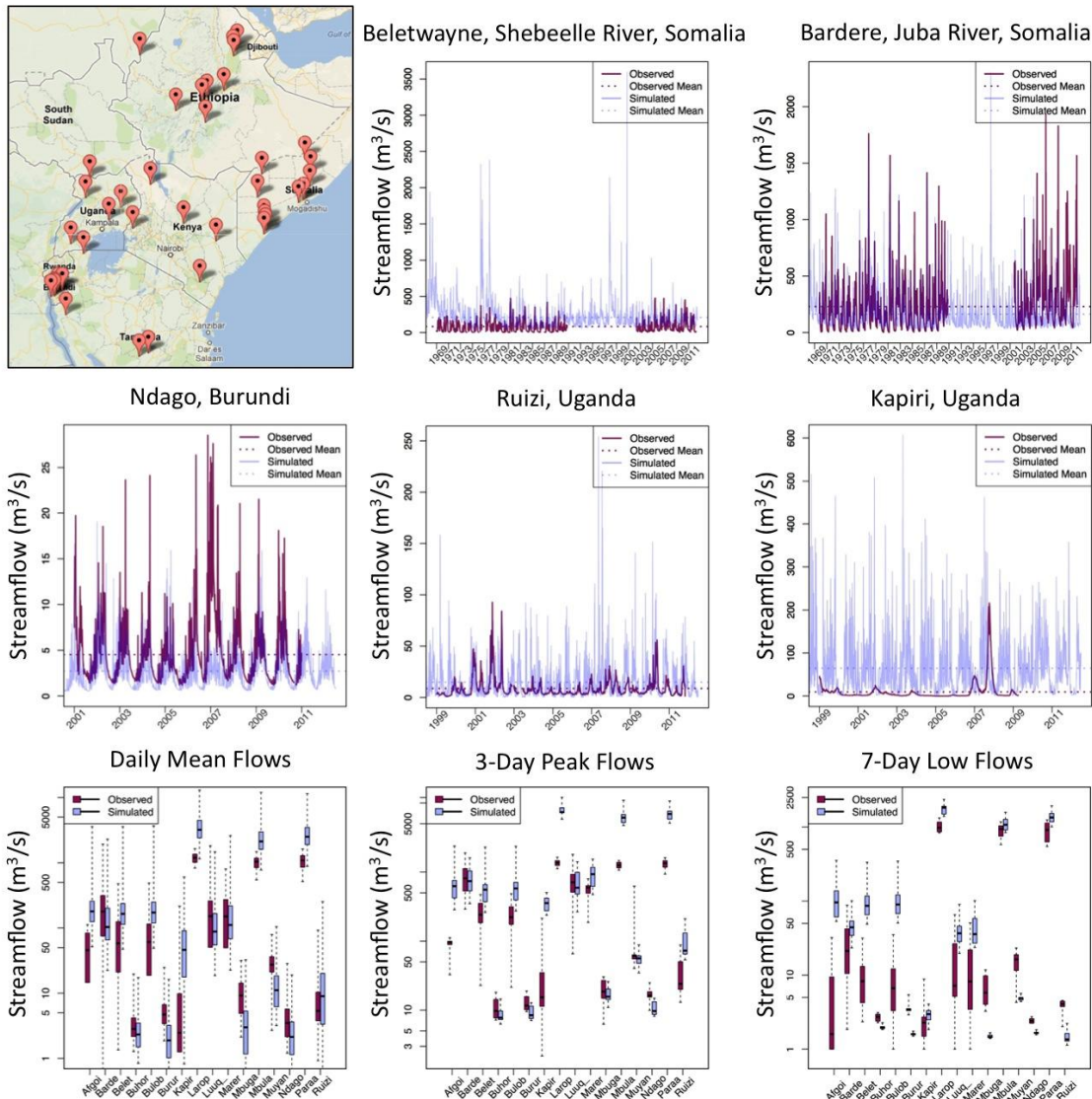


1170

1171 **Figure 5.** (a) A training session at the first workshop in January 2012 at the  
 1172 AGRHYMET center in Niamey, Niger, in which participants from national  
 1173 meteorological and hydrological agencies and river basin management authorities were  
 1174 trained in the use of the system. (b) Participants from the second workshop in June 2012  
 1175 at the ICPAC center in Nairobi, Kenya.



1177 **Figure 6.** Evaluation of VIC model input and output data. Annual mean precipitation  
1178 (mm/day) for 2003-2008 for (a) the TMPA 3B42RT V6 satellite product, (b) the long-  
1179 term (1948-2008) historic ADM data, (c) and their difference (TMPA - ADM). Monthly  
1180 Nash-Sutcliffe efficiency values of the VIC simulated streamflow with respect to  
1181 available historic GRDC observations for (d) the uncalibrated model, (e) the calibrated  
1182 model, and (f) their difference (calibrated – uncalibrated). Annual mean  
1183 evapotranspiration (mm/day) for 1997-2006 for (g) the RS-PM satellite product of  
1184 Vinokullo et al., (2012), (h) VIC, and (i) their difference (VIC – RS-PM). The seasonal  
1185 range in water storage ( $\Delta S$ ; mm) for 2003-2011 for (j) GRACE JPL rel5, (k) VIC, and (l)  
1186 their difference GRACE - VIC.  
1187



1189

1190 **Figure 7.** An example of streamflow validation over the Greater Horn of Africa region

1191 for a diverse set of basins. (top right) location of validation sites selected by participants

1192 from national hydrological agencies at the ICPAC workshop in 2012. (top two rows)

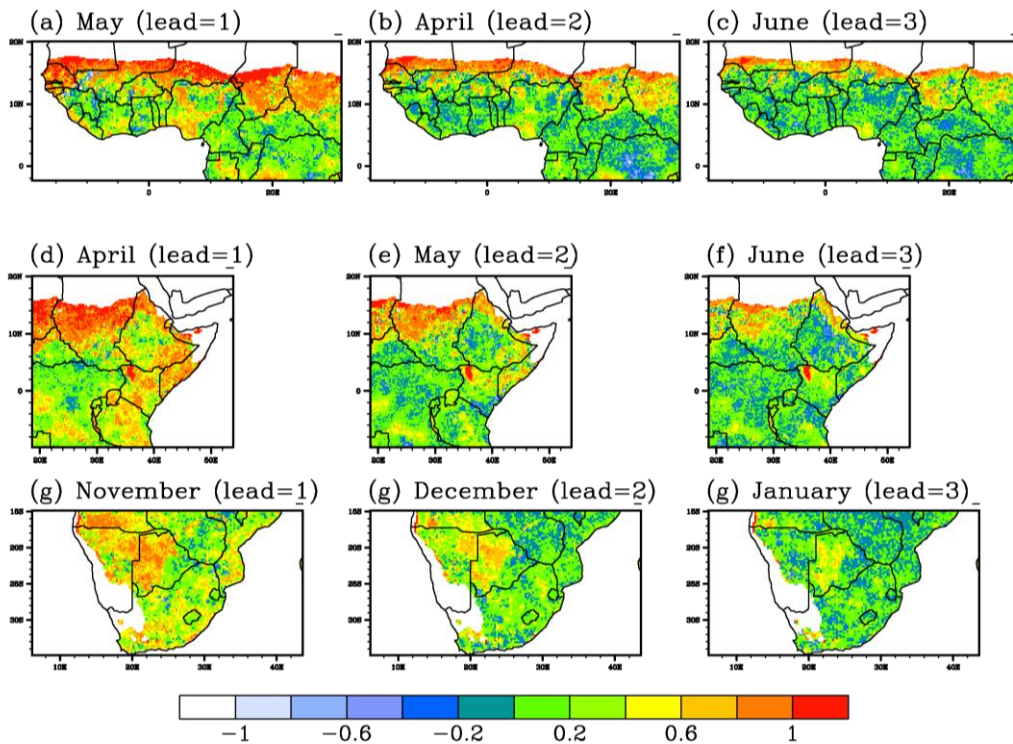
1193 Examples of time series of simulated streamflow discharge from the ADM compared to

1194 available observations. The Beledweyne site is on the Shebeelle River in south-central

1195 Somalia, which is an area of intensive irrigation. The Bardera site is on the Juba River in

1196 southern Somalia, which is an important agricultural area. Note the lack of observational  
1197 data during the peak of the Somali civil war in the 1990s. The Ndago site is in a small  
1198 catchment in southwestern Burundi. The Ruizi site is in southwestern Uganda and may be  
1199 subject to water abstractions. The Kapiri site in eastern Uganda is in a wetland area  
1200 between two lakes. (bottom row) Summary comparisons for 16 sites in Somalia, Uganda  
1201 and Burundi for (left) mean flows, (middle) 3-day peak flows, and (bottom) 7-day low  
1202 flows. The median (horizontal line), inter-quartile range (box) and range (whiskers) are  
1203 shown for the observations and ADM predictions.  
1204

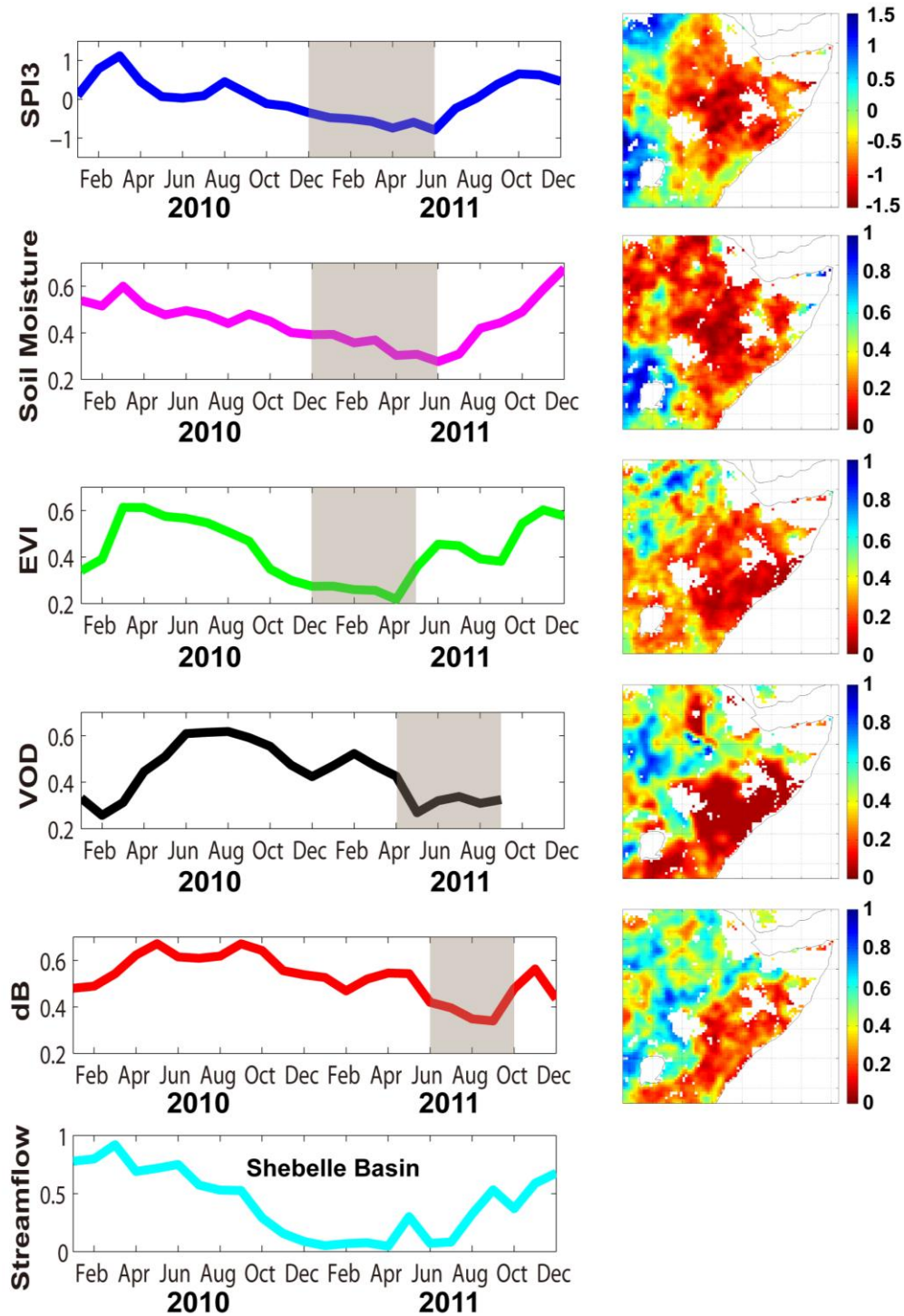
1205



1206

1207 **Figure 8.** Brier skill score for 1, 2 and 3-month forecasts of soil moisture for (a) West  
1208 Africa (forecast date = 15 April), (b) East Africa (forecast date = 15 March) and (c)  
1209 Southern Africa (forecast date = 15 October). The forecasts are from VIC model  
1210 simulated soil moisture forced by bias-corrected and downscaled CFSv2 climate  
1211 forecasts, and evaluated relative to the VIC observation-forced historic simulation. The  
1212 reference forecast is the soil moisture climatology from the offline simulation.

1213



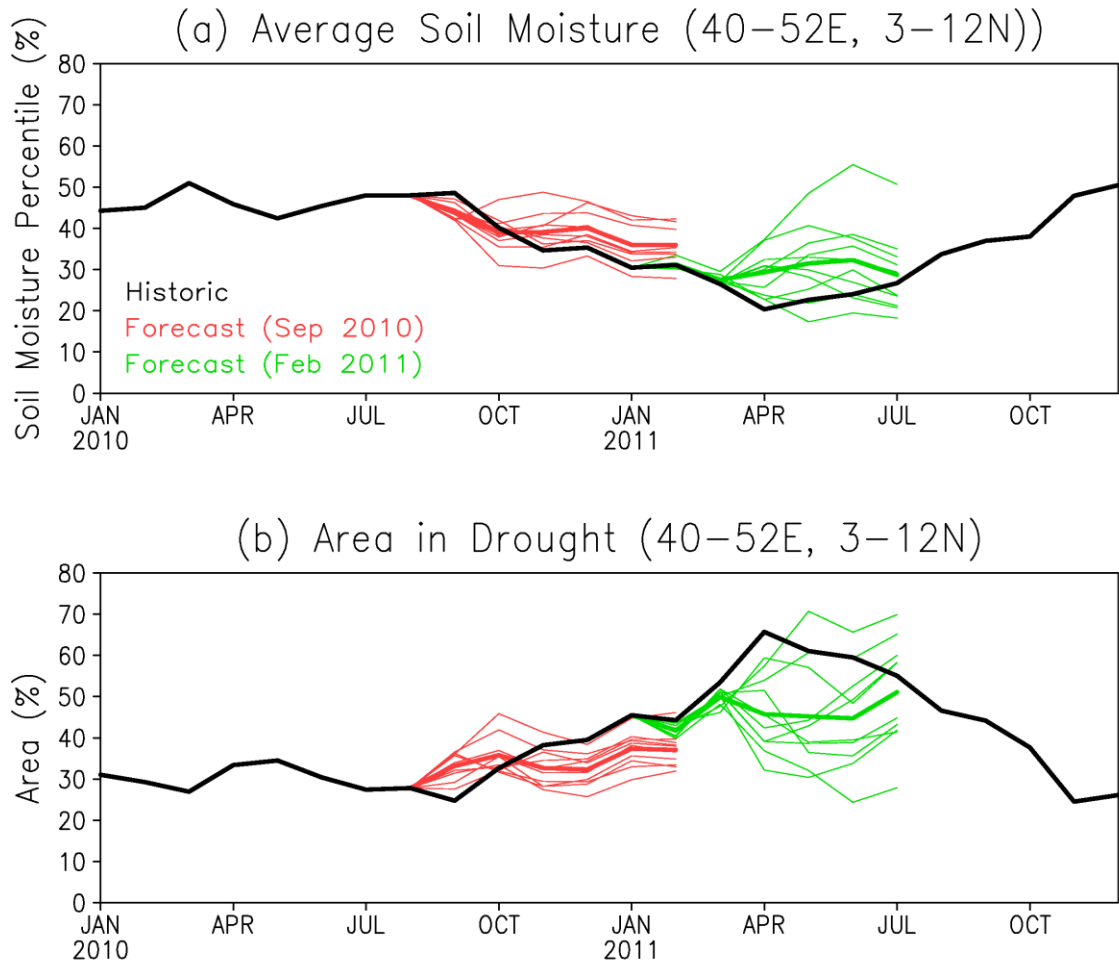
1214

1215 **Figure 9.** The evolution of the 2010-2011 drought over the Horn of Africa. (left) Time

1216 series of drought indices averaged over the HoA region (30-52E, 5S-15N) and (right)

1217 maps of drought indices at the height of the drought as indicated by the gray shading in

1218 the time series. The bottom time series shows the simulated streamflow at the Agfoi  
1219 gauging station on the Shebelle River (upstream area = 107,336 km<sup>2</sup>), which flows from  
1220 the Ethiopian highlands and is one of the two main rivers (along with the Jubba River) in  
1221 southern Somalia. All indices except SPI3 are calculated as percentiles.  
1222



1224

1225 **Figure 10.** Seasonal hydrological forecasts of the 2010/11 Horn of Africa drought. (a)  
 1226 Soil moisture percentile averaged over the main drought region (40-52E, 3-12N) from the  
 1227 historic VIC simulation, September 2010 forecast and February 2011 forecast. (b)  
 1228 Percent area in drought based on a drought threshold of the 20th percentile of soil  
 1229 moisture for the historic simulation and the two forecasts. The forecasts are shown for 10  
 1230 ensemble members and the ensemble mean (thick lines).